Comparison of Brain Strain Magnitudes Calculated Using Head Tracking Impact Parameters and Body Tracking Impact Parameters Obtained from 2D Video

Kayla Larsen

Thesis submitted to the University of Ottawa in partial
Fulfillment of the requirements for the degree of
Master of Science in Human Kinetics

Advisor
Thomas Blaine Hoshizaki, PhD

Committee Members
Allison Clouthier, PhD
Gordon Robertson, PhD

School of Human Kinetics
Faculty of Health Science
University of Ottawa

Acknowledgements

I would like to extend my sincere gratitude to Dr. T. Blaine Hoshizaki for giving me the opportunity and privilege to study in the Neurotrauma Impact Science Laboratory. Thank you for recognizing my academic potential and helping me improve my research skills and abilities.

I would like to thank the members of my research committee, Dr. Allison Clouthier and Dr. Gordon Robertson, for critically reviewing my work and providing valuable feedback to improve my research. Your expertise and knowledge helped to ensure a successful outcome.

I would like to thank Dr. Andrew Post and Dr. Clara Karton for taking the time to help me understand the complexities involved in developing an impactful research study from a simple scientific question. Your input and guidance have helped me grow as a scholar and researcher. I would also like to thank my lab colleagues: Jasmine, Klara, Janie, Luc, Stephanie, Amy, Jarett, and Ben for keeping me inspired and smiling over the years.

I would like to thank my family and friends for the unparalleled love and encouragement they provided throughout this journey. It is through your support that I have demonstrated a tremendous amount of personal growth and academic success. I am grateful to my sister for always giving great advice and guiding me through the winding, yet exciting, path of life. I will forever be indebted to my parents for giving me opportunities and experiences that have shaped and defined who I am today.

Abstract

Relying on signs and symptoms of head injury outcomes has shown to be unreliable in capturing the vulnerabilities associated with brain trauma (Karton & Hoshizaki, 2018). To accommodate the subjectivity of self-reported symptoms, data collection using sensor monitoring and video analysis combined with event reconstruction are used to objectively measure trauma exposure (Tator, 2013; Scorza & Cole, 2019; Hoshizaki et al., 2014). Athletes are instrumented with wireless sensors designed to measure head kinematics during play. However, these systems have not been widely adopted as they are expensive, face challenges with angular acceleration measures, and often require video confirmation to remove false positives. Video analysis of head impacts, in conjunction with physical event reconstruction and finite element (FE) modeling, is also used to calculate tissue level strain. This data collection method requires specialized equipment and expertise. Effective management of head trauma in sport requires an objective, accessible, and quantifiable tool that addresses the limitations associated with current measurement systems. The purpose of this research was to determine if a simplified version of video analysis and event reconstruction using impact characteristics (velocity, location, mass, and compliance) obtained from body tracking could yield similar measures of brain strain magnitude to the standard head tracking method. Ice hockey impacts (x36) that varied in terms of competition level, event type and maximum principal strain (MPS) were chosen for analysis. 2D videos of previously completed head reconstructions were reanalyzed and each event was reconstructed again in the laboratory using impact parameters obtained from body tracking. MPS values were calculated using finite element (FE) modeling and compared to the MPS values from events that were reconstructed using impact parameters obtained from head tracking. The relationship between head and body tracking MPS data and

level of agreement between MPS categories were also assessed. Overall, a significant difference was observed between MPS magnitudes obtained using impact parameters from body and head tracking data from 2D video. When analyzed by event type, only shoulder and glass events demonstrated significant differences in MPS magnitudes. A strong linear relationship was depicted between the two data collection methods and moderate level of agreement between MPS categories was observed, demonstrating that impact characteristics obtained from body tracking and 2D video can be used to measure brain tissue strain.

Table of Contents

List of Figures

List of Tables

Chapter 1: Introduction

1.1 – Problem Statement

Over the past decade, concussions and acquired brain injuries have become public health concerns affecting millions of people across the globe annually (Russell et al., 2017). However, this number is believed to be much greater as a significant number of cases go unrecognized, undiagnosed, and untreated. Head impacts that do not result in immediate symptoms associated with concussion are often termed *sub-concussive*. However, this term implies that the lower threshold limit for concussion is known and that all brain injuries are diagnosed correctly and accurately (McAllister & McCrea, 2017). Only events involving an athlete being diagnosed with a concussion are deemed traumatic. Impacts that do not present immediate symptoms are often neglected from research and clinical treatment. Therefore, there is currently an entire spectrum of brain trauma that is not being monitored or measured.

Evidence has suggested that asymptomatic injuries resulting from lower-energy impacts can nonetheless cause damage when repeated within a short time frame (McAllister & McCrea, 2017). A history of repetitive neurotrauma has been linked to chronic traumatic encephalopathy (CTE), a neurodegenerative disease characterized by an increased accumulation of hyperphosphorylated tau proteins in the brain's sulci and along small blood vessels (McKee et al., 2016). The risk of developing CTE increases with the number of active years participating in the sport and player position, which has been shown to have a significant effect on impact kinematics and the magnitude of deformations within the sulci (Zimmerman et al., 2021). If the frequency and severity of injuries are not documented correctly, there is no way of monitoring or managing impacts that may contribute to neurodegenerative diseases, such as CTE (Broglio et al., 2012; McKee et al., 2016; Montenigro et al., 2017; Kelley et al., 2021).

Measuring head impact magnitude is challenging and requires obtaining impact velocity, location, mass, and surface compliance to predict the dynamic response of the head (Gennarelli et al., 1982, 1987; Zhang et al., 2001; Kleiven, 2003; Pellman et al., 2003a; Post et al., 2013). Head accelerations affect how energy moves through the brain, resulting in neural tissue damage (Kendall et al., 2012a; Karton & Hoshizaki, 2018). Maximum principal strain (MPS) has been identified as an important measure of brain trauma. When compared to peak head accelerations, MPS provides a more complete measure of the brain's mechanical response under various loading conditions (Kleiven, 2007; Zhang et al., 2004; Post & Hoshizaki, 2012).

The symptoms associated with concussion are the basis of the diagnostic process, rendering the initial assessment subjective. It is the responsibility of the athlete, who likely lacks knowledge and proper resources (especially among youth), to recognize signs and symptoms of a brain injury (Gioia, 2015; Giza, 2014; PHAC, 2019). Symptom-based assessments capture individualized outcomes of brain trauma but fail to identify physical injuries (Karton et al., 2021). These assessment tools are not designed to capture the full range of cellular responses associated with brain trauma, nor do they distinguish changes in neuronal structure and chemistry (Karton & Hoshizaki, 2018). Research has reported that neurobiological complications of an injury may still be present, even after the acute symptoms sustained post-impact have resolved (Graham, 2014; Ling et al., 2015). In other words, neurobiological recovery does not necessarily coincide with symptom recovery. Therefore, relying on symptoms alone is not sensitive enough to capture the vulnerabilities associated with brain trauma (Karton & Hoshizaki, 2018).

To address the limitations associated with symptom-based assessments, scientists have investigated quantitative approaches to measuring trauma. Many researchers have instrumented

athletes with wireless and non-invasive sensors to measure head kinematics during play (Rowson et al., 2018). While the majority of these sensors use accelerometers and gyroscopes to measure 6 degrees of freedom (6DOF) kinematics (Beckwith et al., 2007; Mihalik et al., 2007; Hanlon & Bir, 2010; Rowson et al., 2011), they fail to consider other important impact characteristics (i.e. velocity, location, compliance, mass) and often require video confirmation to remove false positives. These devices are not widely adopted, as they are expensive, cumbersome, and are typically used for research purposes. Instrumented helmets and headgear have been shown to underestimate angular acceleration measures, which have been identified as having a strong relationship with resulting brain tissue strain (Zhang et al., 2004; Kleiven, 2006; Kimpara & Iwamoto, 2011; Post & Hoshizaki, 2015; Patton, 2016). Forero Rueda and colleagues (2011) demonstrated a high correlation between angular acceleration and FE model strain outputs, emphasizing the importance of considering this metric when defining injury mechanisms of human brain tissue. Therefore, a monitoring system that does not accurately measure angular acceleration has limited value in impact biomechanics research.

The biggest limitation associated with symptom-based assessments and impact sensors is that they are not representative of tissue level strain. A quantitative approach to measuring brain trauma involves a combination of video analysis, physical reconstruction and finite element (FE) modelling. This method requires extensive video analysis and complex event reconstruction using a surrogate head form to measure the stresses and strains in brain tissue from simulated impacts (Hoshizaki et al., 2014). This approach was developed to address the limitations associated with existing methods and provide an accurate and objective measure of tissue level damage. Although recognized as the gold standard (Schussler et al., 2017) in neurotrauma

research, this method is time-consuming, inaccessible to most individuals, requires proper resources (equipment, computer software, trained users, etc.) and technical skill.

Current methods used to monitor or measure head impact exposure either (1) provide large amounts of data that lacks context in terms of what is causing the trauma or (2) provide comprehensive data that takes a long time to analyze and process. Effective management of head trauma in sport requires an objective, accessible, and quantifiable tool to overcome the limitations associated with current measures. The objective of this study was to determine if a simplified version of video analysis and event reconstruction using impact characteristics (velocity, location, mass, and compliance) obtained from body tracking could yield similar measures of brain strain magnitude to the standard head tracking method. Specifically, this method will involve measuring brain trauma using body tracking information from 2D video to represent head impacts and calculate maximal principal strain for brain tissue. This method has the potential to create an opportunity to measure and manage brain trauma at all levels of sport and provide individuals and organizations with a valid, economical tool that can be used to obtain head trauma information.

1.2 – Research Question

Can impact parameters obtained from body tracking provide accurate brain strain magnitudes?

1.3 – Study Objective

The objective of this study was to determine if a simplified version of video analysis and event reconstruction using impact characteristics (velocity, location, mass, and compliance) obtained from body tracking could yield similar measures of brain strain magnitude to the standard head tracking method.

1.4 – Null Hypotheses

1. There is no significant linear relationship between the head and body tracking MPS data.
2. There is no difference between the MPS magnitudes obtained using impact parameters from body tracking data and head tracking data from 2D video for shoulder impacts.
3. There is no difference between the MPS magnitudes obtained using impact parameters from body tracking data and head tracking data from 2D video for elbow impacts.
4. There is no difference between the MPS magnitudes obtained using impact parameters from body tracking data and head tracking data from 2D video for glass impacts.
5. There is no difference between the MPS magnitudes obtained using impact parameters from body tracking data and head tracking data from 2D video for boards impacts.
6. There is no difference between the MPS magnitudes obtained using impact parameters from body tracking data and head tracking data from 2D video for ice impacts.

1.5 – Significance

Recent technology has introduced a wide array of accessible and powerful digital platforms. Access to video-recording devices, such as smartphones and tablets, has increased significantly over the past decade becoming much more affordable and accurate over the years (DeFroda et al., 2016). In the sports industry, video analysis and analytics are used for body tracking to identify new talent, optimize training programs, inform team selection, and evaluate competition tactics (Passfield & Hopker, 2017). Due to its accessibility, body tracking data has the potential to be applied universally, whether used on the sidelines or for big data analysis. The advantage of using body tracking data is that the body is larger and easier to detect on video

compared to the head thus, eliminating the need to identify specific head impact parameters. For the purposes of this research, body tracking will be compared to head tracking as a means to obtain brain tissue strain. Head kinematics are presently obtained from video analysis to complete a physical event reconstruction, which provides the inputs for finite element modelling to calculate tissue level strain. This process has the potential to be automated using advanced computer capture programs such as Sportlogiq, Skill Corner, Hudl, Playertek, Dartfish, Kinduct, Kinexion and Iceberg. Professional NHL and Junior ice hockey videos will be used in this study; however, this approach has the potential to be used at all levels of competition and contact sports including American football, rugby, and soccer.

Chapter 2: Literature Review

2.1 – Head Impact Magnitude

The magnitude of a head impact can be quantified using peak head acceleration (head motion) or brain deformation (tissue strain). Early biomechanical research demonstrated a correlation between linear and rotational head acceleration and their compounding effects on brain injury. Rowson and colleagues (2012) investigated the concussive tolerance of humans to rotational acceleration using instrumented helmets and suggested that both linear and rotational components of acceleration contribute to injury. Pellman and colleagues (2003b) evaluated concussion biomechanics using a combination of video analysis and laboratory reconstruction of game impacts. They found a relationship between peak linear and rotational accelerations and suggested that concussion was primarily related to linear acceleration. More recent and advanced studies have demonstrated that linear and rotational accelerations are not always correlated and that these instances are largely explained by the nature and characteristics of the impact (Post & Hoshizaki, 2015).

Head impact kinematics (linear and rotational accelerations) describe the motion of the head following an impact, however, brain injury results from the interaction of this movement and underlying tissue (Post & Hoshizaki, 2012). Brain tissue has a low resistance to shear forces (associated with rotation) and a high resistance to compressive forces (associated with translation) (Ommaya, 1968; Ommaya & Hirsch, 1971). Due to the brain's low shear modulus, rotational accelerations create large magnitude strains in the brain and have been reported as the main contributor to concussive injuries (Post & Hoshizaki, 2015). Maximum principal strain is widely used by researchers to assess brain injury outcomes, as it is a metric that closely approximates the tissue level mechanism of concussion (Bain & Meaney, 2000; Zhang et al.,

2004; Kleiven, 2007; Post & Hoshizaki, 2015). Research using an American football dataset reported a high risk of concussive injury occurring between magnitudes of 0.19 and 0.26 for maximum principal strain (Zhang et al., 2004; Kleiven, 2007; Giordano & Kleiven, 2014; Patton et al., 2015). Further research has reported that signal transmission can be affected between strain magnitudes of 0.05 and 0.15 in the absence of structural damage (Margulies & Thibault, 1992; Bain & Meaney, 2000; Singh et al., 2006; Elkin & Morrison, 2007). Karton and colleagues (2020) established MPS categories – based on physiological responses to axonal stretch, reported concussion & sub-concussion, and clinical outcomes – to capture the full spectrum of injury severity that occurs in sport. Very low (< 8%) and low (8-16.9%) magnitudes correspond with the minimum level of injury required to observe minor structural and/or functional changes in the brain. Moderate (17-25.9%) magnitudes correspond with a 50% risk of concussion injury (measured in the grey or white matter). High (26-34.9%) magnitudes are associated with an increased risk of sustaining a concussive-level injury and very high (≥ 35%) magnitudes represent conditions that often result in a loss of consciousness and persistent symptoms (Karton et al., 2020).

2.2 – Impact Parameters

Strain magnitude is influenced by a unique set of impact parameters – impact velocity, location, mass and surface compliance – that dictate the degree of energy transfer to the head and brain (Hoshizaki et al., 2014; Oeur et al., 2014).

2.2.1 – *Impact Velocity*

The relationship between impact velocity and brain injury severity has been documented using movement biomechanics and pathophysiology. A higher impact velocity increases

momentum ($p = m \times v$), which results in greater behavioral and electrophysiological deficits and axonal injury (Yan et al., 2013). Post and colleagues (2013) examined the relationship between impact velocity and peak magnitude strain related to concussion. A pneumatic linear impactor was used to strike a helmeted Hybrid III head form at 5.5, 7.5, and 9.5 m/s (representative of impacts experienced in American football) for centric and non-centric conditions. A finite element model was used to estimate the brain tissue deformations associated with each impact. The helmets demonstrated the greatest protective capacity at 5.5 and 7.5 m/s, whereas impacts delivered at 9.5 m/s showed an increase in risk of injury. These results suggest that changing the impact velocity can influence the magnitude and location of the resulting brain tissue deformation (Post et al., 2013). The objective of a study performed by Oeur and associates (2019) was to examine the effects of impact velocity, surface stiffness, striking mass, and head impact location on peak head response and strain. They found that striking velocity was the most influential parameter on peak MPS in sporting accidents. Given that children and adolescents are smaller and have lower impact velocities, these results could help evaluate the design and performance of headgear to accommodate different sizes, age groups, and skill levels (Oeur et al., 2019).

The current helmet certification standard is designed to protect ice hockey players from traumatic brain injury (TBI), a common injury from falls to the ice (Post et al., 2016; De Grau et al., 2020a). According to the Canadian Standards Association (CSA), ice hockey helmets are evaluated and certified using a monorail drop onto an MEP (modular elastomer programmer) anvil at 4.5 m/s (Canadian Standards Association, 2015). This velocity is reflective of an average fall from an adult height, which only accounts for 7% of concussion cases (Hutchison et al., 2015a; 2015b). Approximately 88% of concussive events in ice hockey are caused by player-to-

player collisions, with shoulder-to-head impacts being the most common event associated with brain injury (Hutchison et al., 2015a; 2015b). Rousseau (2014) analyzed elbow and shoulder (collision) impacts delivered from hockey players to an anthropomorphic head form. The results revealed an average striking velocity of 6.8 m/s and 5.04 to 5.85 m/s for shoulder and elbow impacts, respectively. Therefore, helmet standards should consider the varying velocities and mechanisms in which brain injury occurs in hockey to effectively protect the athlete against the range of compliances in an ice hockey rink (De Grau et al., 2020a).

2.2.2 – *Impact Location*

The influence of impact location on brain tissue strain is not fully defined, however, it has been hypothesized that the brain is more vulnerable to injury from impacts in certain directions or regions (Elkin et al., 2018; Post et al., 2018). Due to the strong association between angular acceleration and strain, it has been suggested that the direction of skull rotation can affect the magnitude of brain tissue deformation (Weaver et al., 2012). Impacts to the side of the head have been shown to produce significantly higher rotational accelerations compared to impacts to the top, front, or back (Mihalik et al., 2012). Linear and rotational acceleration time curve profiles can also be affected differently if the head is impacted in a linear (through the center of mass, centric) or non-linear (not through the center of mass, non-centric, oblique) fashion (Post et al., 2011; Walsh et al., 2012; Fahlstedt et al., 2012; Milne et al., 2013; Clark et al., 2016). Non-centric impacts have been shown to cause higher angular accelerations, which have been linked to diffuse injuries at the tissue level (Gennarelli et al., 1982; King et al., 2003; Zhang et al., 2004; Walsh & Hoshizaki, 2010; Walsh et al., 2011). Specifically, strain responses have been shown to be dominated by rotational acceleration inputs in terms of magnitude and duration, and less affected by linear acceleration inputs (Post et al., 2017). Hua and colleagues

(2015) used a rat model to analyze intracranial responses to various impact parameters in closed head impact (CHI). They reported lateral impacts, compared to central impacts, produced higher peak MPS levels in the cerebrum, hippocampus, and cerebellum (Hua et al., 2015).

2.2.3 – *Effective Mass*

Research has shown that an increase in mass correlates with an increase in peak linear and peak angular acceleration of the head during an impact. Compared to location and velocity, however, mass has a relatively smaller contribution to changes in the dynamic response of the head (Karton et al., 2014; Oeur et al., 2019a). Oeur and colleagues (2018) tested the effects of varying event characteristics using different Hybrid III headforms on a monorail drop tower simulating fall scenarios. With location and compliance held constant, they found that the combined effects of an increase in impact mass and velocity resulted in the larger adult Hybrid III headform producing concussive level peak angular acceleration and strains at a lower velocity compared to the smaller 6-year-old child and a 5^{th}-percentile female Hybrid III headform (Oeur et al., 2018). Karton and colleagues (2014) examined the effects of inbound mass on the dynamic impact response and brain tissue deformation. To achieve various inbound masses (4.3 kg; 6.3 kg; 8.3 kg; 10.3 kg; 12.3 kg; 14.3 kg), metal plates were fastened to the cylinder of a pendulum and impacts were delivered to a 50^{th} percentile Hybrid III head form under centric and non-centric conditions. The results demonstrated that as inbound mass increased, peak linear accelerations for both conditions also increased. However, peak rotational acceleration responses and peak tissue deformation variables (maximum principal strain and peak von Mises stress) were more variable and dependent on the location of the impact (Karton et al., 2014). These results demonstrate that mass is an important parameter to consider when performing injury

reconstructions, evaluating head protection standards, and assessing the risk of injury (Karton et al., 2014).

2.2.4 – *Surface Compliance*

In a recent study, De Grau and colleagues (2020a) examined the effects of surface compliance on the dynamic response and brain tissue strains during ice hockey impacts. Three striking caps of low, medium, and high compliance were used to strike five impact locations on a Hybrid III headform at three different velocities. They found that as impact compliance increased, the magnitudes of MPS decreased (De Grau et al., 2020a). However, this decrease still posed a risk for concussive injury, even at the lowest impact velocity of 4.5 m/s (Zhang et al., 2004; Kleiven, 2007; Patton et al., 2015). These results were expected, as low-compliance materials deform easily and transfer little energy to the head form. As compression increases, the duration of the impact increases, and the magnitude of rotational acceleration decreases, which ultimately results in less damaging brain tissue strains (Gennarelli, 1983; Willinger et al., 1994; Gilchrist, 2003). One method of enhancing a helmet's ability to reduce peak linear acceleration is to increase its material compliance by adjusting the foam type, size, and stiffness. However, Rousseau (2014) reported that longer-duration impacts can cause high magnitude strains due to the viscoelastic properties of brain tissue. Therefore, increasing the compliance of the materials within the helmet can also increase impulse durations, which has been shown to increase risk of injury (Rousseau, 2014).

2.3 – Event Reconstruction Using Head Impact Parameters

Event reconstruction has been shown useful in defining the link between impact parameters and brain injury (Doorly 2006; 2009; Post et al., 2012). This method involves acquiring a detailed description of the impact from video, reconstructing the event using a

surrogate head and/or neck form equipped with accelerometers, and examining strain responses from finite element modeling (O'Riordain et al., 2003; Post et al., 2012). Impact reconstructions provide important information regarding the head's dynamic response (linear & rotational accelerations) and brain tissue deformation (strains and stresses), which can help researchers understand the relationship between these metrics and injury outcomes (Doorly, 2006; 2009; Kleiven, 2007; Post et al., 2012; Willinger & Baumgartner, 2003; Zhang et al., 2004).

Video analysis involves obtaining detailed characteristics (velocity, location, compliance, mass) of the head impact and measuring velocity using video analysis software, such as Kinovea (www.Kinovea.org, open source). Videos of sports games (across many levels of play) have been used to quantify the mechanisms of injury and describe head trauma outcomes. This footage is typically of the highest quality with multiple camera views (wide-angle, sideline, etc.) of every play. Information and details regarding playing surface, injury play, player-to-player interaction, primary helmet impact source and location can be determined through video analysis (Lessley et al., 2018). To determine a precise head impact location, videos of the impact are cropped, viewed from multiple angles, and observed in slow motion. A grid reference system is typically used to identify the contact area on the helmet or head form (Ignacy, 2017; Post et al., 2019a; Karton et al., 2020). For head injury reconstructions, it is important to have accurate representations of the varying surfaces that a player can impact during a game or practice. The compliance for each surface represents a different level of stiffness and translates into graded peak acceleration/time pulse durations between 5 and 30 ms (Post et al., 2019a). Head-to-ice impacts are represented by low compliance short-duration events and correspond with duration pulses of 10 to 22.7 ms and MPS values of 0.34 to 0.70 (Post et al., 2019a; Meehan, 2019; De Grau et al., 2020a). Head-to-boards impacts are similar in that they result in duration pulses of

12.6 to 26 ms and have MPS values that range from 0.32 to 0.40 (Post et al, 2019a; Meehan 2019). Head-to-shoulder impacts are representative of high compliance long-duration events and correspond with duration pulses of 18 to 27.5 ms and MPS values of 0.20 to 0.33 (Rousseau, 2014; Post et al., 2019a; Meehan, 2019; De Grau et al., 2020a). Elbow impacts result in similar loading conditions to those of the shoulder, as they both involve limb-to-head interactions. These events have duration pulses of 10 to 28 ms and MPS values of 0.18 to 0.38 (Rousseau, 2014; Post et al., 2019a; De Grau et al., 2020a). Post and colleagues (2019a) reported moderate compliance levels for head-to-glass impacts that correspond with a duration range of 15 to 20 ms and an average MPS of 0.21 (Appendix B: Table 24). Mass has also been shown to have an influence on rotational kinematics and strain metrics. For instances where a player has fallen to the ice or crashed into the boards or glass, the mass of the Hybrid III head form and neck form (6.08 kg) are used for reconstruction purposes. The mass used to reconstruct shoulder (13.1 kg) and elbow (5.2 kg) impacts correspond with the mass of the test equipment used to simulate each event (Rousseau 2014; Rousseau & Hoshizaki, 2015).

To obtain linear and rotational time histories from head impacts, events must be reconstructed using a surrogate head and/or neck form and mechanical test equipment. Currently, many head form variations can be used for head impact simulation and helmet testing. The Hybrid III head form is commonly used for impact reconstruction because it is durable enough to sustain multiple high magnitude impacts without breaking and has a 3-2-2-2 accelerometer set-up array that collects three-dimensional dynamic response measurements. This instrumentation is necessary for finite element (FE) analysis, which requires adequate loading curves to calculate brain tissue stresses and strains (Padgaonkar et al., 1975; Kendall et al., 2012b). Once detailed impact characteristics are collected from video analysis, impacts are delivered to the head form

using a linear impactor, monorail drop rig, or pendulum. The linear impactor is used to reconstruct player collisions and consists of a standing frame that supports a pneumatically accelerated impacting arm. Once engaged, the impacting arm projects toward the head form, which is mounted on a sliding table that moves with little resistance post-impact (Hoshizaki et al., 2014; Kosziwka et al., 2021). Depending on the mass and mechanism of injury, the pendulum can also be used to reconstruct player collisions. This system consists of a hollow, free-swinging frame suspended by aviation cables that are fastened to a metal beam directly above the head form (Karton et al., 2014). The monorail drop rig is used to reconstruct falls and consists of a drop carriage and 4.7 m long rail guided by bushings to reduce the influence of friction on inbound velocity measurements (Clark et al., 2018b). For each system, various striking caps and anvils can be used to represent the unique compliance conditions associated with ice hockey impacts (Oeur et al., 2019; Post et al., 2019a). After impacting the helmeted head form, the resulting dynamic response curves are inputted into an FE model to calculate brain tissue strain (De Grau et al., 2020a).

2.4 – Finite Element Modelling

Finite element (FE) models of the human brain allow researchers to study brain injury in an ethical manner, as they do not require experimentation on live human subjects or cadavers (Trotta et al., 2020). A validated model can be used to predict, simulate, or reconstruct brain injuries that occur from sports and accidents. Specifically, these models can provide the extent of stress and strain undergone by the brain during an impact, which are better indicators of injury compared to linear and rotational accelerations (Yang & King, 2011). The University College Dublin Brain Trauma Model (UCDBTM) was developed by Horgan and Gilchrist in 2003 and was recently modified and improved (UCDBTM V2.0) by Trotta and colleagues in 2020. These

refinements include: (1) updating the mechanical properties of several components of the head to reflect recent experimental studies, (2) introducing a low coefficient of friction between the scalp and skull to accurately depict sliding properties, (3) modifying the mesh of the model to increase the number of elements from 28,268 to 184,261, and (4) incorporating accelerometer elements at the center of gravity of the model to allow for a direct comparison between linear and rotational head accelerations (Trotta et al., 2020). After the model was validated using cadaver data, the kinematics, stresses, and strains of the UCDBTM V1.0 and V2.0 models were compared using three real-world concussion cases from equestrian riding falls (Clark et al., 2018a; Trotta et al., 2020). Compared to the UCDBTM V1.0, the UCDBTM V2.0 demonstrated an increase in the relative rotation of the head with respect to the helmet and predicted high peak levels of stress and strain that coincided with the concussion values reported in literature (Clark et al., 2018a).

2.5 – Player Tracking

To develop safe game play, coaches require a means of identifying factors that lead to unfavorable outcomes (i.e. brain injury). Current coaching tools, such as sports analytics, are more commonly used to identify favorable outcomes such as game success (Kniffin et al., 2017). Professional sports teams invest in advanced predictive analytics and other areas of advanced data analysis in hopes of achieving a competitive advantage (Greenbaum, 2018). The goal of this research is to determine if similar datasets can be used to identify game play characteristics that measure an athlete's risk of injury. A user-friendly, inexpensive and interactive tracking program could be used to follow athletes or group of athletes during game play and capture head impact events from 2D video. Sports tracking systems provide positional, velocity, and acceleration data for the players and playing objects (Seidl et al., 2016). Most systems have been shown to accurately document athletes' on-field activity, but as the play moves faster with less linear

movements, the accuracy and reliability of these technologies tends to decrease (Buchheit et al., 2014). Obtaining high-definition video provides better image resolution, makes it easier to detect and confirm head impacts and obtain more accurate measurements. However, storing a large volume of data related to impact characteristics present additional challenges. Big data technologies provide solutions for storing these large datasets and facilitate the process of accessing this information through various interfaces (Rein & Memmert, 2016).

The study of brain injury biomechanics would merit from the application of player tracking technology to head impact event reconstruction. Small objects, such as a helmet, can be difficult to track using an automated system and without the use of embedded sensors or infrared technology (Cotsonika, 2020; Ogus, 2020; Lage, 2021). The affordability and accessibility of 2D video would facilitate the manner in which brain strain measurements are obtained. Instead of analyzing the video in great detail to identify specific head impact characteristics, the player's body could be used to make generalized and rational assumptions regarding the event. Ice hockey players are often in an upright and neutral position, especially when performing crossovers to minimize their displacement around a circular path. The head, shoulders, and torso are stacked over the skater's center of gravity and the player uses their legs to achieve the highest level of performance (McClelland, 2021). During a heading event in soccer, the head and shoulders move in unison with the torso during contact with the ball for purposes of redirection (clearing, passing, or gaining control) (Shewchenko et al., 2005). Since accelerations are tangential to the head, it can be assumed that an impact to the upper torso and shoulders would affect the head in a similar manner and that a general head impact location could be assigned based on observed body orientation (Mihalik et al., 2012). Additionally, compliance could be made more generalized by grouping events that involve similar contact surfaces. Identifying

contact surfaces using video analysis can be challenging and time-consuming, particularly if the video footage is of lesser quality or there was only one angle of view. Grouping shoulder and elbow impacts into player collisions, and boards and ice impacts into falls, would eliminate the need to identify a precise impact location.

Bailey and colleagues (2020) examined the accuracy of a videogrammetry (the study of obtaining 3D measurements from 2D video images) technique to track the position and rotation of the helmet before, during and after a head impact. The rationale for this study was based on the accessibility of broadcasted game video at the professional level and the advancements and improvements in the quality of videography in terms of frame rate and resolution. Their method was successful in quantifying helmet velocity over a longer period of time, in more degrees of freedom, and with greater accuracy than previous work (Bailey et al, 2020). Gyemi and colleagues (2021) also used a video-based tracking method to describe impact mechanisms, estimate 3D pre-impact velocities, and impact-induced velocity changes. Results from this study demonstrate the value of implementing body tracking technology to compute three-dimensional helmet kinematics and improve brain injury assessments and helmet test standards (Gyemi et al., 2021).

Chapter 3: Methodology

3.1 – Overview

The objective of this study was to determine whether impact parameters collected using body tracking can be used to predict brain strain magnitude. Body tracking describes the temporal association between human detections (all instances where a human is present in an image) within a video sequence to generate trajectories (Davis et al., 2019). Since specific vectors and refined impact characteristics are challenging to obtain by video observation alone, the aim was to use impact characteristics that an automated tracking system could presumably detect to simplify the current method while maintaining an objective and accurate measure of brain tissue deformation. MPS values from the head tracking method were compared the body tracking method to determine whether these simplified parameters are just as influential in measuring brain strain magnitude.

3.2 – Hybrid III Head Form and Neck Form

To simulate on-field impacts, laboratory reconstructions (reenactments) of the impact were conducted with a helmeted 50th-percentile Hybrid III head form and unbiased neck form (Figure 1A). The Hybrid III 50th-percentile adult male head form and neutral unbiased neck form was equipped with nine Endevco 7264C-2KTZ-2-300 accelerometers arranged in a 3-2-2-2 array (Padgaonkar et al., 1975). The neck form was composed of 171.2 mm diameter aluminum disks separated by four butyl elastomer layers and a braided steel cable ran through the center to add strength and support to the system (Walsh et al., 2018). The head form was fitted with a CCM Tacks 110 Senior Hockey Helmet (Figure 1B), which contains an improved multi-density foam liner that was developed to help manage a variety of impacts (CCM Hockey, 2021).

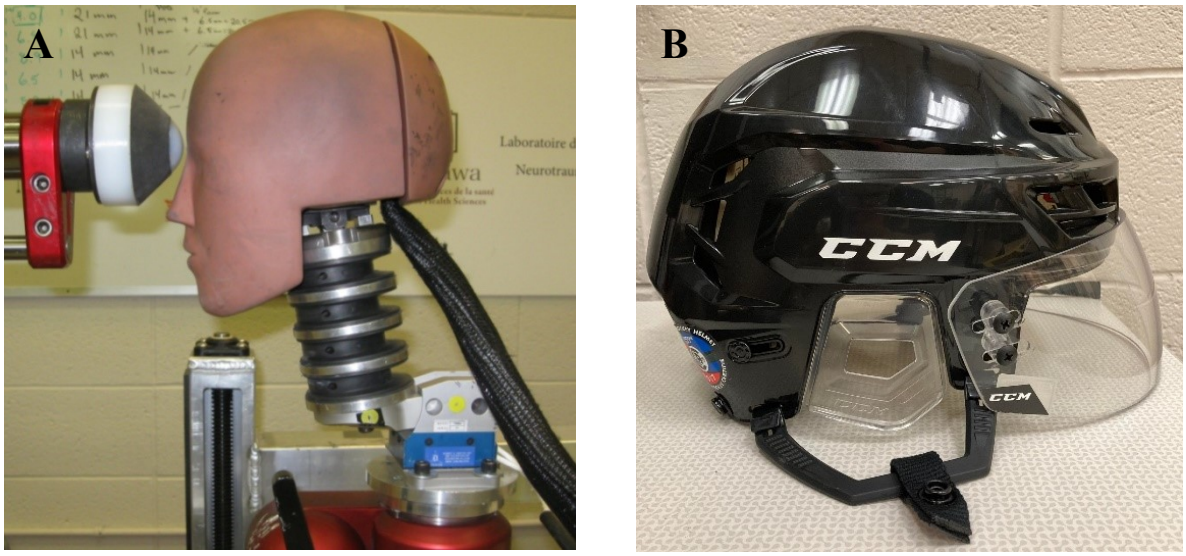

Figure 1. *(A) Hybrid III head and neck form mounted to the sliding table on the pneumatic linear impactor and (B) CCM Tacks 110 Senior Hockey Helmet*

3.3 – Video Analysis

Videos (recorded at 25 frames/sec) of previously completed head reconstructions were reanalyzed to eliminate any subjective bias in velocity measurements. Impacts (x36) that varied in terms of competition level (Junior and NHL), event type and MPS were chosen for analysis. For the head tracking method, an accurate and detailed view of the impact location was determined using video manipulation (multiple video angles, slow motion, close-up/zoom features) and a grid reference system to identify the contact area on the helmet (Figure 2). For the body tracking method, a generalized impact location (front, side, and rear) based on observed body orientation was used for reconstruction purposes. Once the moment of impact was identified, the motion of the head or body was tracked for 2-5 frames pre-impact to establish the displacement. A perspective grid was applied to the playing surface and calibrated using reference markings (blue line, face off dots etc.) and dimensions that correspond with a standard NHL hockey rink. For shoulder and elbow impacts, two vertical lines were drawn from the: (1)

impact location of the head or body and (2) contacting surface, to the ground. An arrow was used to join the bottom ends of the two vertical lines and the distance measured between them was divided by the time (t = 0.2 s for 5 frames) to obtain impact velocity. Depending on the camera angle and body orientation, the center of the sternum (front impacts), scapulae (rear impacts), or glenohumeral joint (side impacts) was used as a reference point to calculate velocity for the body tracking method. For example, the center of the scapulae would have been used as a reference point if the player was facing away from the camera and only their rear was visible. The same method was used to calculate velocity for glass and boards impacts, except that a marker was placed on the object where the head was going to impact, and the vertical line was drawn from this point. For falls to the ice, the motion of the head or body was tracked for 2 frames pre-impact to establish the displacement and only one vertical line was drawn from the impact location to the ground. Vertical impact velocity was calculated by dividing the distance by the time (t = 0.08 s for 2 frames) (Appendix A). For the head and body tracking methods, velocity was measured twice to increase accuracy and reliability.

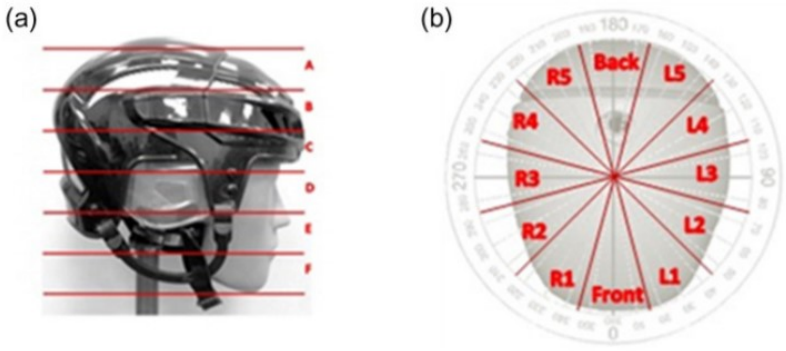

Figure 2. *Grid reference system used to identify specific head impact locations; obtained from Post et al., 2019a*

3.4 – Event Reconstruction

3.4.1 – *Head Tracking Reconstruction Method*

Depending on the event type, the mechanical equipment, anvils, and striking caps used to reconstruct each event varied (Table 1; Figure 3; Figure 4). The pneumatic linear impactor consists of an impacting arm and a large frame (Figure 3A). The impacting arm consists of an air canister, frame, and an aluminum shaft (13.1 ± 0.1 kg). The large frame has a sliding table (12.78 ± 0.01 kg) with an attachment site for the head form, which allows for movement post-impact (Karton et al., 2020). Shoulder-to-head impacts were conducted in a similar manner to Rousseau and Hoshizaki's (2015) work using a linear impactor system. The impacting end of the of the linear impactor was fitted with a piece of 0.11 m thick VN 602 foam covered with a 0.025 m tall rounded VN cap and a Reebok 11 K shoulder pad (Figure 4A) (Rousseau, 2014). Elbow-to-head impacts were conducted using the pendulum system with an elbow anvil, which was comprised of an aluminum frame covered in a piece of ¼ inch vinyl nitrile 602 foam with an RBK11k elbow pad (Figure 3B; Figure 4B) (Rousseau 2014; Rousseau and Hoshizaki 2015). A monorail drop rig was used to simulate crashes to the glass and falls to the boards & ice (Figure 3C). The Hybrid III head and neckform was attached to a guided rail system via a holding carriage. This unit was dropped from a predetermined height onto a frozen anvil (Figure 4E) to replicate the surface compliance of a hockey rink (Post et al., 2019a; Karton et al., 2020). A steel anvil supporting a round piece of high-density polyethylene (0.012 m thick) was used to reconstruct head-to-boards impacts (Figure 4D). Similarly, a large 1.83 m by 1.22 m (0.012 m thick) piece of polycarbonate glass, secured by a wooden frame, was used to reconstruct head-to-glass impacts (Figure 4C).

Table 1. *Test equipment and anvils used to reconstruct head impacts using the head tracking reconstruction method*

Event	Shoulder	Elbow	Glass	Boards	Ice
Equipment[1,2]	Linear Impactor	Pendulum	Monorail Drop Rig	Monorail Drop Rig	Monorail Drop Rig
Anvil	High compliance striker cap with shoulder pad	Elbow striker with elbow pad	Polycarbonate glass	Flat steel anvil with high density polyethylene	Frozen ice anvil

Note. [1] Post et al., 2019a; [2] Meehan, 2019

Figure 3. *Test equipment used to reconstruct head impact events: (A) pneumatic linear impactor, (B) pendulum, and (C) monorail drop rig*

Figure 4. *Anvils used to represent different contact surfaces for the head tracking reconstruction method: (A) shoulder, (B) elbow, (C) glass, (D) boards, and (E) ice*

3.4.2 – *Body Tracking Reconstruction Method*

After reconstructing each event three times using head impact parameters, events were reconstructed again using the body tracking reconstruction method (Table 2). Assuming that player tracking and analytics programs are unable to detect specific head impact parameters, nor identify the orientation of an athlete during an impact, head impact reconstructions were conducted using less-refined body tracking information. A generalized event type (collision, crash, fall) and impact location (front, side, and rear) of the body were used for reconstruction purposes. Shoulder-to-head and elbow-to-head impacts were conducted using the pneumatic linear impactor (Figure 3A). Rousseau (2014) reported a wide range of shoulder-to-head impact durations that varied from 18 to 32 ms. Post and colleagues (2019a) found that elbow events also varied considerably in their durations, from 10 to 28 ms. Therefore, the impacting end of the of the linear impactor was fitted with a medium compliance striker cap (Figure 5A) which was designed to produce an average impact duration of 25 ms, which is reflective of the average durations reported in literature (Appendix B: Table 25). This cap consisted of a 0.065 m thick layer of 405S DER-TEX foam (DERTEX Corp., Saco, ME, USA) covered with a 0.025 m tall rounded VN cap. Similar to the research conducted by Meehan (2019), head-to-ice and head-to-boards impacts were conducted using the monorail drop rig. The helmeted head form was positioned on a rectangular drop carriage, which was then raised and dropped from a predetermined height onto a flat steel anvil covered with a cylindrical MEP pad (Figure 5B) to replicate low compliance surface conditions. The carriage landed on a braking system, which allowed the head form to respond freely post-impact. Compared to boards and ice, head-to-glass impacts create different loading characteristics for the helmeted head. Therefore, these events were assigned to their own category and a more compliant anvil was used for reconstruction

purposes. Due to the nature of these impacts, reconstructions were conducted in the same manner to those obtained using the head tracking reconstruction method, which used the monorail drop rig and a large 1.83 m by 1.22 m (0.012 m thick) piece of polycarbonate glass.

Figure 5. *Anvils used to represent different contact surfaces for the body tracking reconstruction method: (A) shoulder & elbow, (B) boards & ice*

Table 2. *Test equipment and anvils used to reconstruct head impacts using the body tracking reconstruction method*

Event	Collisions (Shoulder & Elbow)	Glass	Falls (Boards & Ice)
Equipment	Linear Impactor	Monorail Drop Rig	Monorail Drop Rig
Anvil	Medium compliance striker cap	Polycarbonate glass	Flat MEP anvil

3.5 – Finite Element Model

After each event was reconstructed in the laboratory three times, an MPS value was obtained using the University College Dublin Brain Trauma Model V2.0 (Trotta et al., 2020) (Figure 6). The UCDBTM V2.0 contains 184,261 elements and was validated using adult cadaver head research conducted by Loyd et al. (2014) and Hardy et al. (2001, 2007). The mechanical properties of this model can be found in Table 3. Brain strain responses were calculated using the three-dimensional head motion dynamic response (acceleration-time) curves obtained from the physical reconstructions and applied to the centre of gravity of the FE model (Figure 7). MPS magnitudes were then assigned to one the following categories: very low = < 8%, low = 8-16.9%, moderate = 17-25.9%, high = 26-34.9% and very high = ≥ 35% (Karton et al., 2020) (Figure 8).

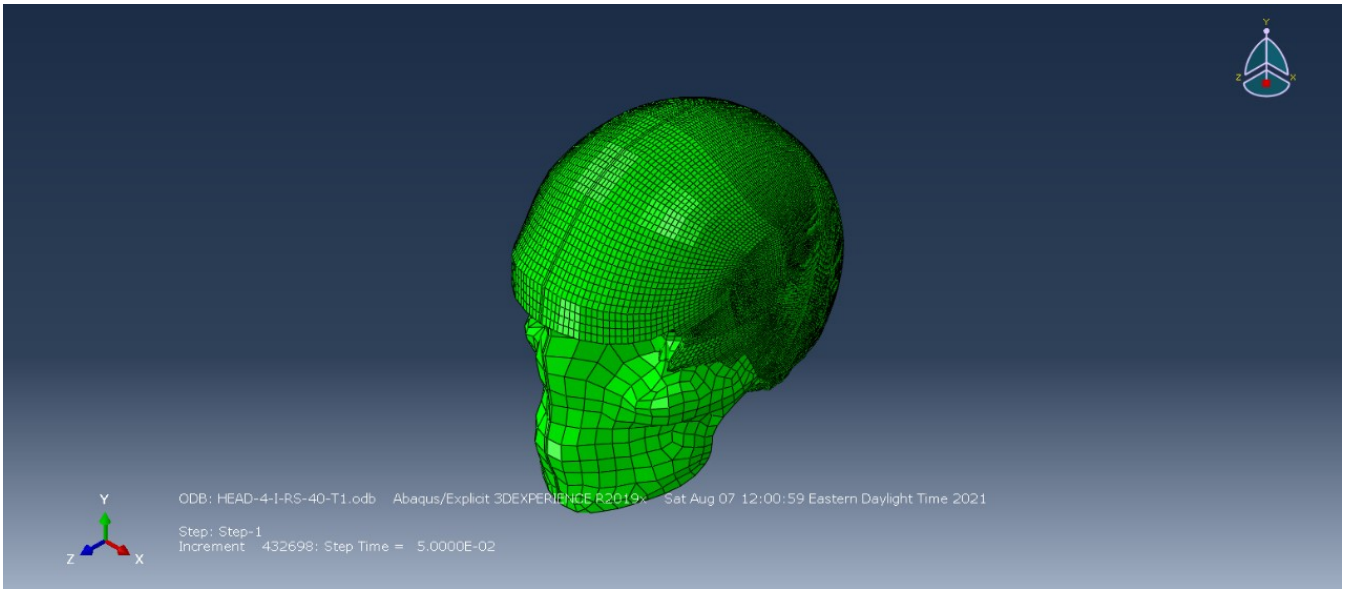

Figure 6. *Example of the University College Dublin Brian Trauma Model V2.0*

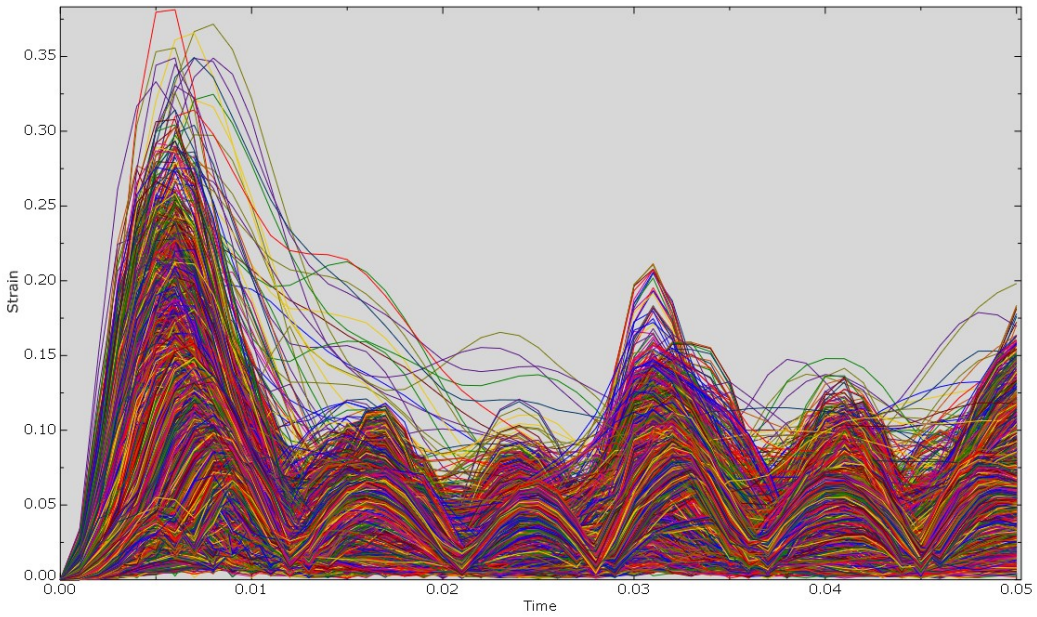

Figure 7. *Example of the brain strain time histories for the grey matter elements in the University College Dublin Brain Trauma Model V2.0*

Table 3. *Summary of the mechanical properties used in the UCDBTM V2.0; obtained from Trotta et al., 2020*

Region	Model	Density (kg/m^3)	Poisson's Ratio
Scalp	Hyperelastic	1133	~ 0.5
Cerebellum	Visco-hyperelastic	1060	~ 0.5
Grey matter	Visco-hyperelastic	1060	~ 0.5
Brainstem	Visco-hyperelastic	1060	~ 0.5
Cortical bone	Linear elastic	2000	0.22
Trabecular bone	Linear elastic	1300	0.24
Pia	Linear elastic	1130	0.45
CSF	Linear elastic	1000	~ 0.5
Facial bone	Linear elastic	2100	0.22
Ventricles	Visco-hyperelastic	1040	~ 0.5
White matter	Viscoelastic	1060	~ 0.5
Dura, falx, and tentorium	Hyperelastic	1130	~ 0.5

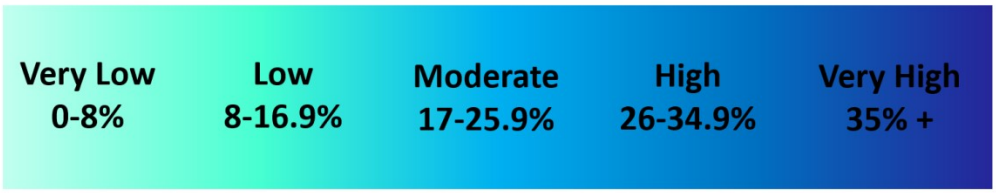

Figure 8. *Five MPS magnitude categories used to capture entire spectrum of trauma in sport; obtained from Karton et al., 2020*

3.6 – Statistical Analysis

All statistical analyses were performed using Microsoft Excel or Jamovi 2.2.5. For the head and body tracking methods, velocity was measured twice (four times total) to improve accuracy. Pearson correlations and paired t-tests were used to determine if the first and second rounds of velocity measurements for the two methods were significantly different and correlated (test re-test reliability). Linear regressions were used to determine if there was a significant linear relationship between head and body tracking MPS data (overall & for each event type). A repeated-measures ANOVA was performed to determine if MPS magnitudes differed significantly between the head and body tracking methods across the five event types, and paired t-tests were used to determine where these significant differences occurred. Weighted Cohen's kappa (κ) was used to measure the interrater reliability (level of agreement) between MPS categories. An alpha level of .05 was used for all statistical analyses, except when multiple comparisons were performed. For these instances, a Bonferroni correction was used to reduce the probability of committing a type I error.

Chapter 4: Results

Tables 4, 5, 6, 7, and 8 demonstrate the impact parameters (location and velocity) documented from video analysis and the equipment used to reconstruct shoulder, elbow, glass, boards, and ice impacts. Using the head tracking method, location and elevation was determined using a grid reference system, which divided the helmeted head into 12 sectors and 6 levels and was obtained from Post and colleagues (2019a). For the body tracking method, the orientation of the hockey player's body was observed, and a general location was assigned. The anvils (compliance) and equipment used to reconstruct each event were predetermined and based on previous research studies (Rousseau, 2014; Post et al., 2019a; Meehan, 2019; De Grau et al., 2020a). For both methods, velocity was measured using Kinovea video analysis software using the head or body (center of the sternum, scapulae, or glenohumeral joint) as a reference point. The first and second rounds of velocity measurements were strongly correlated, with Pearson correlation coefficients of R = .988 and R = .984, for the head and body tracking methods respectively. Using the Bonferroni correction ($\alpha_{adjusted} = .05/2 = .025$), no significant differences in velocity measurements were observed for the head tracking ($t(35) = 2.22$, $p = 0.03$) and body tracking ($t(35) = 1.48$, $p = .147$) methods.

Table 4

Impact parameters (obtained from video analysis) used to reconstruct shoulder-to-head impacts using the two data collection methods

Event	Head					Body			
	Location	**Elevation**	**Velocity (m/s)**	**Compliance (anvil)**	**Equipment**	**Location**	**Velocity (m/s)**	**Compliance (anvil)**	**Equipment**
Shoulder 1	Front boss	R1-D	4.23	High with shoulder pad	Linear impactor	Front	4.49	Medium compliance	Linear impactor
Shoulder 2	Right side	R2-F	4.76	High with shoulder pad	Linear impactor	Side	5.15	Medium compliance	Linear impactor
Shoulder 3	Left side	L4-E	5.26	High with shoulder pad	Linear impactor	Side	5.78	Medium compliance	Linear impactor
Shoulder 4	Right side	R2-F	5.65	High with shoulder pad	Linear impactor	Side	6.21	Medium compliance	Linear impactor
Shoulder 5	Left side	L2-D	7.28	High with shoulder pad	Linear impactor	Side	7.50	Medium compliance	Linear impactor
Shoulder 6	Right side	R3-D	7.28	High with shoulder pad	Linear impactor	Side	7.81	Medium compliance	Linear impactor
Shoulder 7	Right side	R4-D	8.33	High with shoulder pad	Linear impactor	Side	9.35	Medium compliance	Linear impactor
Shoulder 8	Front boss	L1-E	8.71	High with shoulder pad	Linear impactor	Front	9.35	Medium compliance	Linear impactor

Table 5

Impact parameters (obtained from video analysis) used to reconstruct elbow-to-head impacts using the two data collection methods

Event	Head					Body			
	Location	Elevation	Velocity (m/s)	Compliance (anvil)	Equipment	Location	Velocity (m/s)	Compliance (anvil)	Equipment
Elbow 1	Left side	L2-E	1.99	Elbow striker & elbow pad	Pendulum	Side	2.63	Medium compliance	Linear impactor
Elbow 2	Left side	L2-D	4.61	Elbow striker & elbow pad	Pendulum	Side	5.37	Medium compliance	Linear impactor
Elbow 3	Right side	R4-D	4.61	Elbow striker & elbow pad	Pendulum	Side	5.02	Medium compliance	Linear impactor
Elbow 4	Right side	R3-B	4.94	Elbow striker & elbow pad	Pendulum	Side	5.30	Medium compliance	Linear impactor
Elbow 5	Rear	BACK-E	5.14	Elbow striker & elbow pad	Pendulum	Rear	5.26	Medium compliance	Linear impactor
Elbow 6	Front	FRONT - E	5.39	Elbow striker & elbow pad	Pendulum	Front	6.26	Medium compliance	Linear impactor
Elbow 7	Front boss	L1-E	6.39	Elbow striker & elbow pad	Pendulum	Front	6.58	Medium compliance	Linear impactor

Table 6

Impact parameters (obtained from video analysis) used to reconstruct shoulder-to-head impacts using the two data collection methods

Event	Head					Body			
	Location	**Elevation**	**Velocity (m/s)**	**Compliance (anvil)**	**Equipment**	**Location**	**Velocity (m/s)**	**Compliance (anvil)**	**Equipment**
Glass 1	Right side	R3-C	3.08	Polycarbonate glass	Drop rig	Side	3.56	Polycarbonate glass	Drop rig
Glass 2	Front	FRONT-A	3.24	Polycarbonate glass	Drop rig	Front	3.27	Polycarbonate glass	Drop rig
Glass 3	Front boss	L1-B	3.49	Polycarbonate glass	Drop rig	Front	4.26	Polycarbonate glass	Drop rig
Glass 4	Front boss	R1-C	3.58	Polycarbonate glass	Drop rig	Front	4.66	Polycarbonate glass	Drop rig
Glass 5	Left side	L3-B	3.90	Polycarbonate glass	Drop rig	Side	4.66	Polycarbonate glass	Drop rig
Glass 6	Right side	R2-C	4.20	Polycarbonate glass	Drop rig	Side	4.95	Polycarbonate glass	Drop rig
Glass 7	Front	FRONT-C	4.26	Polycarbonate glass	Drop rig	Front	5.25	Polycarbonate glass	Drop rig
Glass 8	Right side	R2-C	4.52	Polycarbonate glass	Drop rig	Side	5.22	Polycarbonate glass	Drop rig

Table 7

Impact parameters (obtained from video analysis) used to reconstruct boards-to-head impacts using the two data collection methods

Event	Head					Body			
	Location	**Elevation**	**Velocity (m/s)**	**Compliance (anvil)**	**Equipment**	**Location**	**Velocity (m/s)**	**Compliance (anvil)**	**Equipment**
Boards 1	Rear	BACK-D	1.64	Flat anvil & high-density polyethylene	Drop rig	Rear	2.88	Flat MEP anvil	Drop rig
Boards 2	Rear	BACK-E	2.30	Flat anvil & high-density polyethylene	Drop rig	Rear	2.81	Flat MEP anvil	Drop rig
Boards 3	Right side	R3-C	3.54	Flat anvil & high-density polyethylene	Drop rig	Side	4.52	Flat MEP anvil	Drop rig
Boards 4	Left side	L2-B	4.34	Flat anvil & high-density polyethylene	Drop rig	Side	4.52	Flat MEP anvil	Drop rig
Boards 5	Rear	BACK-E	5.76	Flat anvil & high-density polyethylene	Drop rig	Rear	6.56	Flat MEP anvil	Drop rig
Boards 6	Left side	L2-B	6.05	Flat anvil & high-density polyethylene	Drop rig	Side	6.48	Flat MEP anvil	Drop rig

Table 8

Impact parameters (obtained from video analysis) used to reconstruct ice-to-head impacts using the two data collection methods

Event	Head					Body			
	Location	Elevation	Velocity (m/s)	Compliance (anvil)	Equipment	Location	Velocity (m/s)	Compliance (anvil)	Equipment
Ice 1	Rear	BACK-C	3.39	Ice anvil	Drop rig	Rear	4.37	Flat MEP anvil	Drop rig
Ice 2	Rear	BACK-D	3.48	Ice anvil	Drop rig	Rear	3.91	Flat MEP anvil	Drop rig
Ice 3	Front boss	L1-B	3.65	Ice anvil	Drop rig	Front	4.07	Flat MEP anvil	Drop rig
Ice 4	Right side	R3-D	4.07	Ice anvil	Drop rig	Side	4.96	Flat MEP anvil	Drop rig
Ice 5	Rear	BACK-D	4.33	Ice anvil	Drop rig	Rear	4.80	Flat MEP anvil	Drop rig
Ice 6	Left side	L4-C	4.55	Ice anvil	Drop rig	Side	5.25	Flat MEP anvil	Drop rig
Ice 7	Rear	BACK-C	5.06	Ice anvil	Drop rig	Rear	5.19	Flat MEP anvil	Drop rig

4.1 – Overall

A simple linear regression was performed to investigate the overall relationship between head and body tracking. The scatterplot showed a significant and positive linear relationship, which was confirmed with a Pearson's correlation coefficient of .918 and an R^2 of .842 ($F(1, 34) = 181.18$, $p < .001$) (Figure 9). Figure 10 demonstrates an overall comparison of the MPS magnitudes obtained using the head and body tracking methods and a significant difference was observed ($t(35) = -3.43$, $p = .002$). A repeated-measures ANOVA determined that mean MPS values differed significantly across the five event types ($F(1, 34) = 11.7$, $p = .002$). A post hoc pairwise comparison using the Bonferroni correction ($\alpha_{adjusted} = .05/5 = .01$) showed significant differences in MPS magnitudes obtained using the two methods for shoulder ($t(7) = -8.15$, $p < .001$) and glass ($t(7) = -3.91$, $p = .006$) events (Figure 11). The two methods demonstrated a significant and moderate level of agreement (56%) between MPS categories overall, with a weighted Cohen's kappa value of 0.56 ($p < .001$) (Table 9).

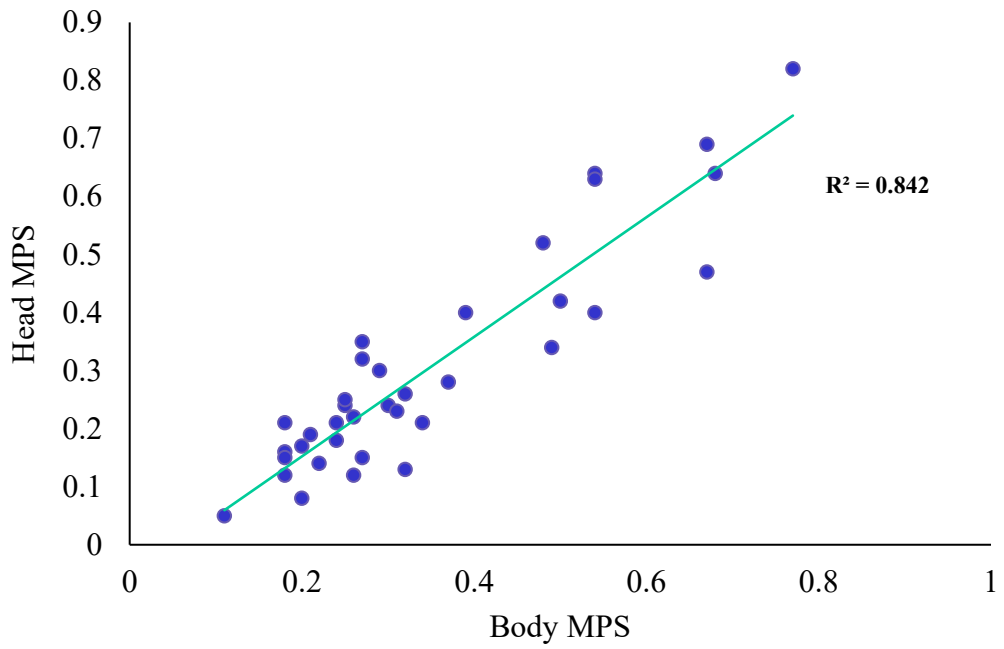

Figure 9. *Scatterplot and regression line demonstrating the overall relationship between head and body MPS*

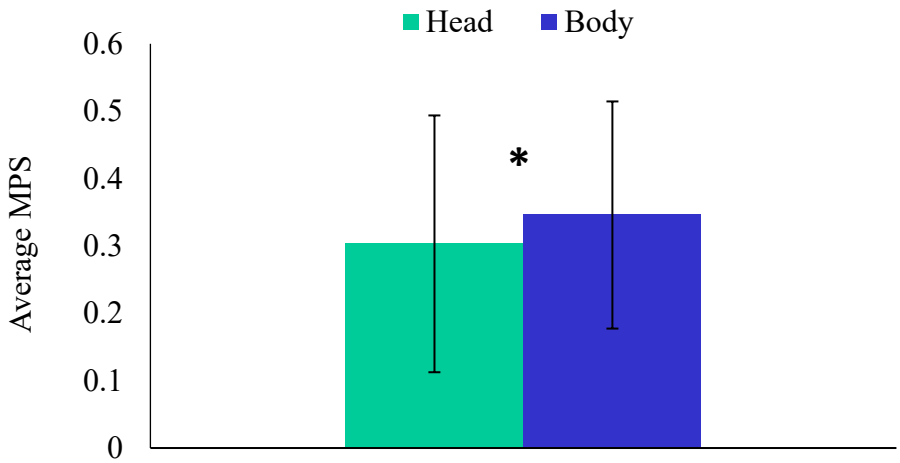

Figure 10. *Overall comparison between the average MPS magnitudes obtained using the head and body tracking methods; asterisks (*) indicate significant differences and error bars represent standard deviation*

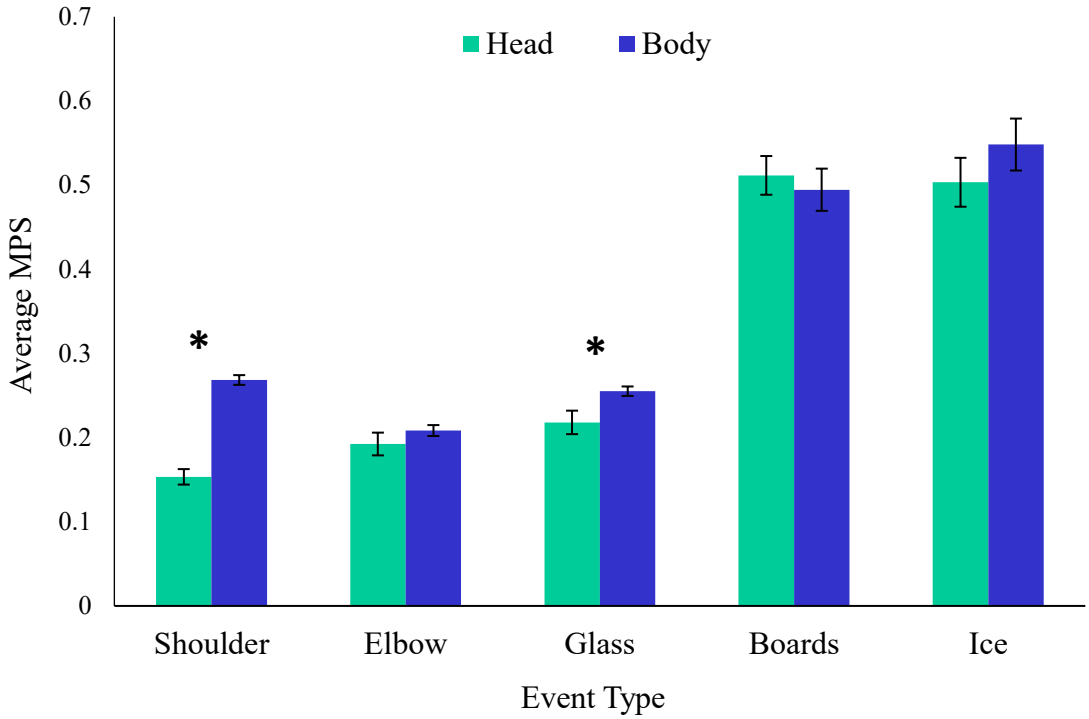

Figure 11. *Average MPS magnitudes for shoulder, elbow, glass, boards, and ice impacts; asterisks (*) indicate significant differences and error bars represent standard deviation*

Table 9. Weighted *Cohen's kappa and percent agreement values for MPS categories obtained from head and body tracking reconstructions*

Event Type	Cohen's Kappa (κ)	Cohen's Kappa Interpretation	% Agreement	*P*-Value
Shoulder	0.06	Slight	0	0.41
Elbow	0.36	Fair	43	0.02
Glass	0.29	Fair	63	0.17
Boards	1.00	Almost perfect	100	0.01
Ice	0.00	Poor	86	1.00
Overall	0.56	Moderate	56	< .001

Note. Interpretation of kappa values (level of agreement) was proposed by Landis & Koch, 1977

4.2 – Shoulder

For the head tracking method, shoulder impacts were reconstructed using the linear impactor with a high compliance striker cap and shoulder pad (Table 4). All impacts were delivered to the front boss, right side, or left side locations and the velocities ranged from 4.23 m/s to 8.71 m/s. The MPS values ranged from 8% to 28%, none of which fell within the very high MPS category (Table 12).

For the body tracking method, the same impacts were reconstructed using the linear impactor with a medium compliance striker cap (Table 4). Impacts were either delivered to the front or side of the head and the velocities ranged from 4.49 m/s to 9.35 m/s. The MPS values ranged from 20% to 37%, none of which fell within the very low and low MPS categories (Table 12).

The average velocities for the head and body tracking methods were 6.44 m/s and 6.96 m/s, respectively. The average difference in velocity for the two methods was 0.52 m/s (Table 10). The dynamic responses for all shoulder impacts can be found in Table 11. The average MPS values for the head and body tracking methods were 0.15 and 0.27, respectively (Table 12 and Figure 12). Shoulder events did not demonstrate a statistically significant level of agreement (0%) between MPS categories for the two methods ($\kappa = 0.06$, $p = .41$) (Table 9). Shoulder events demonstrated a significant linear relationship between head and body MPS data, but had the lowest R^2 value of .66 ($F(1, 6) = 11.90$, $p = .01$) (Figure 13).

Table 10. *Average difference in velocity between the head and body tracking reconstruction methods for shoulder impacts*

Event	Head Velocity (m/s)	Body Velocity (m/s)	Difference (m/s)
Shoulder 1	4.23	4.49	0.25
Shoulder 2	4.76	5.15	0.39
Shoulder 3	5.26	5.78	0.52
Shoulder 4	5.65	6.21	0.56
Shoulder 5	7.28	7.50	0.22
Shoulder 6	7.28	7.81	0.53
Shoulder 7	8.33	9.35	1.02
Shoulder 8	8.71	9.35	0.64
Average	**6.44**	**6.96**	**0.52**

Table 11. *Impact locations, velocities, and linear and rotational accelerations for shoulder impacts reconstructed using the head and body tracking data collection methods*

Event	Head				Body			
	Location	Velocity (m/s)	Linear Acceleration (g)	Rotational Acceleration (rad/s^2)	Location	Velocity (m/s)	Linear Acceleration (g)	Rotational Acceleration (rad/s^2)
Shoulder 1	Front Boss	4.23	10.13	616.00	Front	4.49	23.40	1373.67
Shoulder 2	Right Side	4.76	11.30	1360.53	Side	5.15	24.40	2049.60
Shoulder 3	Left Side	5.26	11.83	854.67	Side	5.78	30.47	2290.60
Shoulder 4	Right Side	5.65	10.73	2096.97	Side	6.21	32.57	2704.57
Shoulder 5	Left Side	7.28	22.90	2224.70	Side	7.50	42.50	2996.50
Shoulder 6	Right Side	7.28	23.43	1420.97	Side	7.81	45.33	3501.30
Shoulder 7	Right Side	8.33	16.47	2036.43	Side	9.35	57.33	4637.03
Shoulder 8	Front Boss	8.71	16.00	3722.73	Front	9.35	46.20	3063.70

Table 12. *Average MPS magnitudes and categories obtained from FE analysis of shoulder impacts*

Event	Head		Body	
	MPS	MPS Category	MPS	MPS Category
Shoulder 1	0.08	Very Low	0.20	Moderate
Shoulder 2	0.12	Low	0.18	Moderate
Shoulder 3	0.12	Low	0.26	High
Shoulder 4	0.14	Low	0.22	Moderate
Shoulder 5	0.21	Moderate	0.34	High
Shoulder 6	0.15	Low	0.27	High
Shoulder 7	0.13	Low	0.32	High
Shoulder 8	0.28	High	0.37	Very High
Average	0.15	-	0.27	-

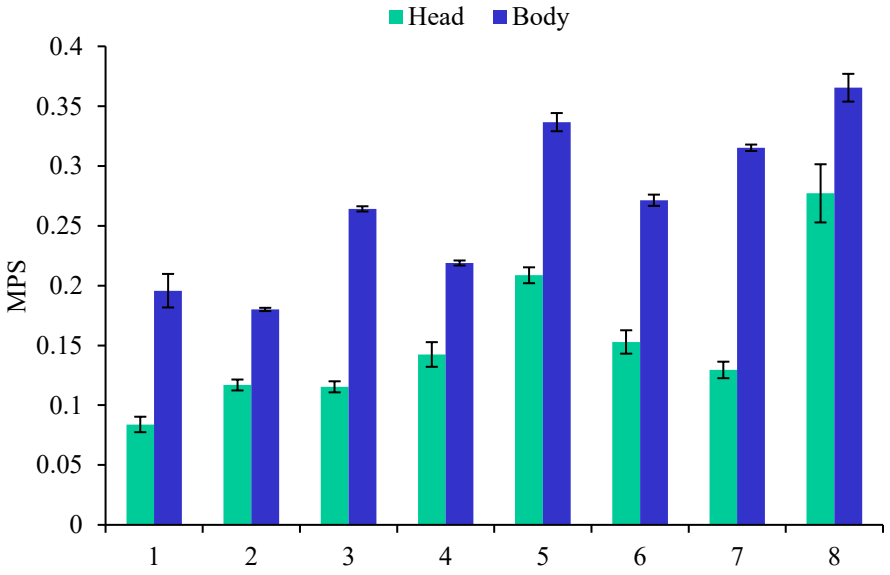

Figure 12. *Average MPS magnitudes obtained using the UCDBTM V2.0 for shoulder impacts reconstructed head and body tracking impact parameters; error bars represent the standard deviation of the three reconstruction trials performed for each event*

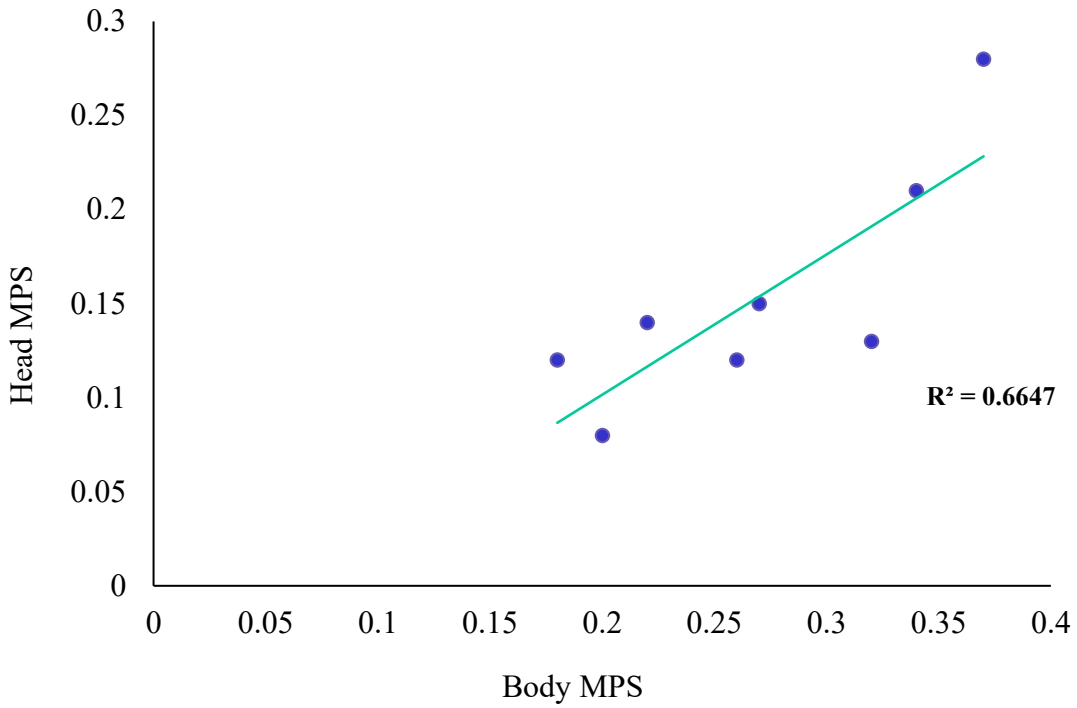

Figure 13. *Scatterplot and regression line demonstrating the relationship between head and body MPS for shoulder events*

4.3 – Elbow

For the head tracking method, elbow impacts were reconstructed using the pendulum with an elbow striker and elbow pad (Table 5). Impacts were delivered to the right & left side, rear, front, and front boss locations and the velocities ranged from 1.99 m/s to 6.39 m/s. The MPS values ranged from 5% to 35%, four of which fell within the moderate MPS category (Table 15).

For the body tracking method, the same impacts were reconstructed using the linear impactor with a medium compliance striker cap (Table 5). Impacts were delivered to the side, rear, and front locations and the velocities ranged from 2.63 m/s to 6.58 m/s. The MPS values ranged from 11% to 27%, four of which fell within the moderate and none of which fell within the very high MPS category (Table 15).

The average velocities for the head and body tracking methods were 4.72 m/s and 5.20 m/s, respectively. The average difference in velocity for the two methods was 0.48 m/s (Table 13). The dynamic responses for all elbow impacts can be found in Table 14. The average MPS values for the head and body tracking methods were 0.19 and 0.21, respectively (Table 15 and Figure 14). The two methods demonstrated a significant and fair level of agreement (43%) between MPS categories, with a weighted Cohen's kappa value of 0.36 (p = .02) (Table 9). Elbow events demonstrated a significant linear relationship between head and body MPS data and had an R^2 value of .71 ($F(1, 5) = 12.51$, p = .02) (Figure 15).

Table 13. *Average difference in velocity between the head and body tracking reconstruction methods for elbow impacts*

Event	Head Velocity (m/s)	Body Velocity (m/s)	Difference (m/s)
Elbow 1	1.99	2.63	0.64
Elbow 2	4.61	5.37	0.76
Elbow 3	4.61	5.02	0.41
Elbow 4	4.94	5.30	0.36
Elbow 5	5.14	5.26	0.12
Elbow 6	5.39	6.26	0.87
Elbow 7	6.39	6.58	0.19
Average	**4.72**	**5.20**	**0.48**

Table 14. *Impact locations, velocities, and linear and rotational accelerations for elbow impacts reconstructed using the head and body tracking data collection methods*

Event	Head				Body			
	Location	Velocity (m/s)	Linear Acceleration (g)	Rotational Acceleration (rad/s^2)	Location	Velocity (m/s)	Linear Acceleration (g)	Rotational Acceleration (rad/s^2)
Elbow 1	Left Side	1.99	3.83	654.80	Side	2.63	10.77	790.47
Elbow 2	Left Side	4.61	20.50	1597.07	Side	5.37	27.43	2061.00
Elbow 3	Right Side	4.61	21.10	2429.20	Side	5.02	24.03	2060.37
Elbow 4	Right Side	4.94	30.40	2711.23	Side	5.30	25.90	2175.20
Elbow 5	Rear	5.14	26.33	1741.77	Rear	5.26	25.83	1882.43
Elbow 6	Front	5.39	26.90	3122.10	Front	6.26	30.60	2059.73
Elbow 7	Front Boss	6.39	49.17	7341.20	Front	6.58	31.30	2100.17

Table 15. *MPS values and categories obtained from FE analysis of elbow impacts*

Event	Head		Body	
	MPS	MPS Category	MPS	MPS Category
Elbow 1	0.05	Very Low	0.11	Low
Elbow 2	0.18	Moderate	0.24	Moderate
Elbow 3	0.16	Low	0.18	Moderate
Elbow 4	0.21	Moderate	0.18	Moderate
Elbow 5	0.19	Moderate	0.21	Moderate
Elbow 6	0.22	Moderate	0.26	High
Elbow 7	0.35	Very High	0.27	High
Average	0.19	-	0.21	-

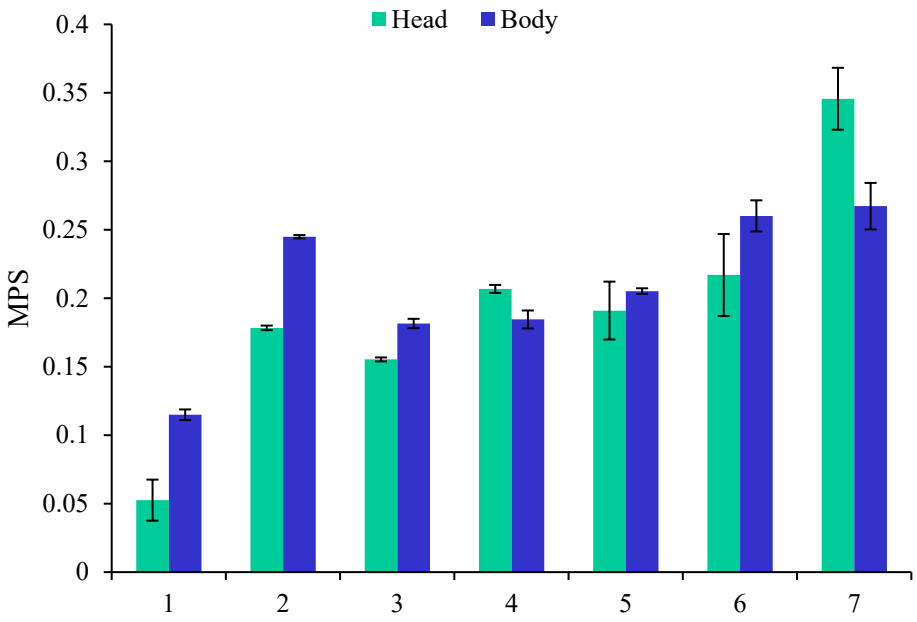

Figure 14. *MPS magnitudes obtained using the UCDBTM V2.0 for elbow impacts reconstructed using parameters obtained from head and body tracking; error bars represent the standard deviation of the three reconstruction trials performed for each event*

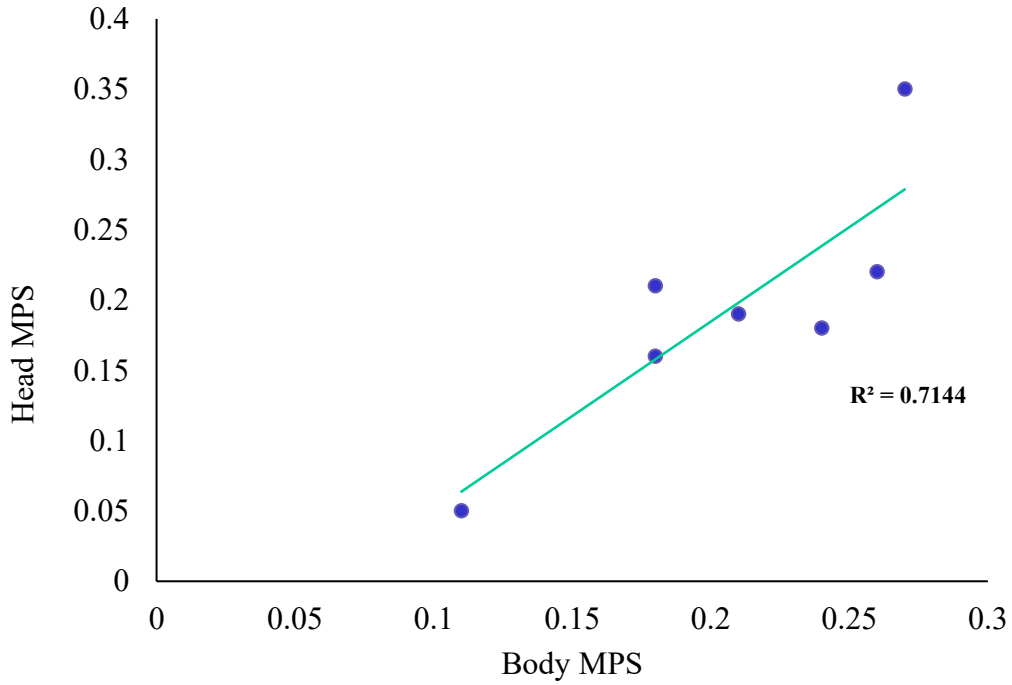

Figure 15. *Scatterplot and regression line demonstrating the relationship between head and body MPS for elbow events*

4.4 – Glass

For the head tracking method, impacts were delivered to the left & right side, front, and front boss locations and the velocities ranged from 3.08 m/s to 4.52 m/s. The MPS values ranged from 15% to 25%, six of which fell within the moderate MPS category (Table 18).

For the body tracking reconstruction method, impacts were either delivered to the side or front locations and the velocities ranged from 3.56 m/s to 5.22 m/s. The MPS values ranged from 18% to 25%, all of which fell within the moderate or high MPS categories (Table 18).

For the head and body tracking methods, glass impacts were reconstructed using the monorail drop rig and polycarbonate glass (Table 6). Although the reconstruction mechanism remained consistent between the two methods, the velocities and locations varied. The average velocities for the head and body tracking methods were 3.78 m/s and 4.48 m/s, respectively. The average difference in velocity for the two methods was 0.70 m/s (Table 16). The dynamic responses for all glass impacts can be found in Table 17. The average MPS values for the head and body tracking methods were 0.22 and 0.26, respectively (Table 18 and Figure 16). Glass events did not demonstrate a statistically significant level of agreement (63%) between MPS categories for the two methods ($\kappa = 0.29$, $p = .17$) (Table 9). However, glass events demonstrated a significant linear relationship between head and body MPS data and had an R^2 value of .72 ($F(1, 6) = 15.64$, $p = .008$) (Figure 17).

Table 16. *Average difference in velocity between the head and body tracking reconstruction methods for glass impacts*

Event	Head Velocity (m/s)	Body Velocity (m/s)	Difference (m/s)
Glass 1	3.08	3.56	0.49
Glass 2	3.24	3.27	0.03
Glass 3	3.49	4.26	0.77
Glass 4	3.58	4.66	1.07
Glass 5	3.90	4.66	0.77
Glass 6	4.20	4.95	0.75
Glass 7	4.26	5.25	0.99
Glass 8	4.52	5.22	0.70
Average	**3.78**	**4.48**	**0.70**

Table 17. *Impact locations, velocities, and linear and rotational accelerations for glass impacts reconstructed using the head and body tracking data collection methods*

Event	Head				Body			
	Location	Velocity (m/s)	Linear Acceleration (g)	Rotational Acceleration (rad/s^2)	Location	Velocity (m/s)	Linear Acceleration (g)	Rotational Acceleration (rad/s^2)
Glass 1	Right Side	3.08	34.77	2889.30	Side	3.56	48.37	4520.53
Glass 2	Front	3.24	36.53	3430.53	Front	3.27	32.77	1813.03
Glass 3	Front boss	3.49	30.13	1939.60	Front	4.26	51.13	2725.40
Glass 4	Front boss	3.58	37.80	2704.07	Front	4.66	44.87	2715.83
Glass 5	Left Side	3.90	41.40	3535.95	Side	4.66	51.20	4309.30
Glass 6	Right Side	4.20	39.17	2201.00	Side	4.95	66.13	5566.97
Glass 7	Front	4.26	46.30	1888.53	Front	5.25	57.07	2861.47
Glass 8	Right Side	4.52	64.07	6212.87	Side	5.22	61.10	4919.33

Table 18. *MPS values and categories obtained from FE analysis of glass impacts*

Event	Head		Body	
	MPS	**MPS Category**	**MPS**	**MPS Category**
Glass 1	0.15	Low	0.18	Moderate
Glass 2	0.17	Moderate	0.20	Moderate
Glass 3	0.21	Moderate	0.24	Moderate
Glass 4	0.24	Moderate	0.25	Moderate
Glass 5	0.24	Moderate	0.30	High
Glass 6	0.26	High	0.32	High
Glass 7	0.23	Moderate	0.31	High
Glass 8	0.25	Moderate	0.25	Moderate
Average	0.22	-	0.26	-

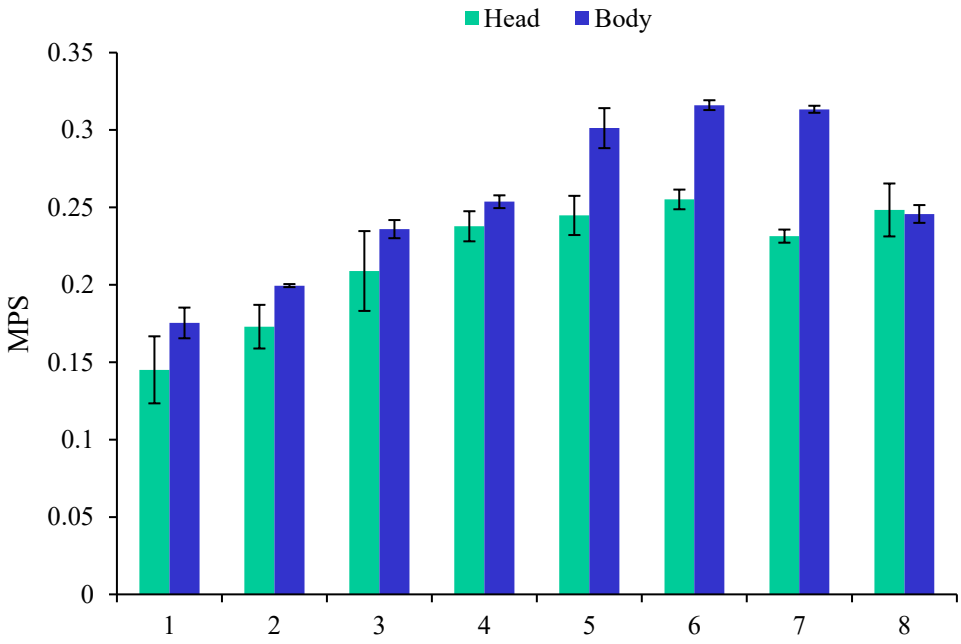

Figure 16. *MPS magnitudes obtained using the UCDBTM V2.0 for glass impacts reconstructed using parameters obtained from head and body tracking; error bars represent the standard deviation of the three reconstruction trials performed for each event*

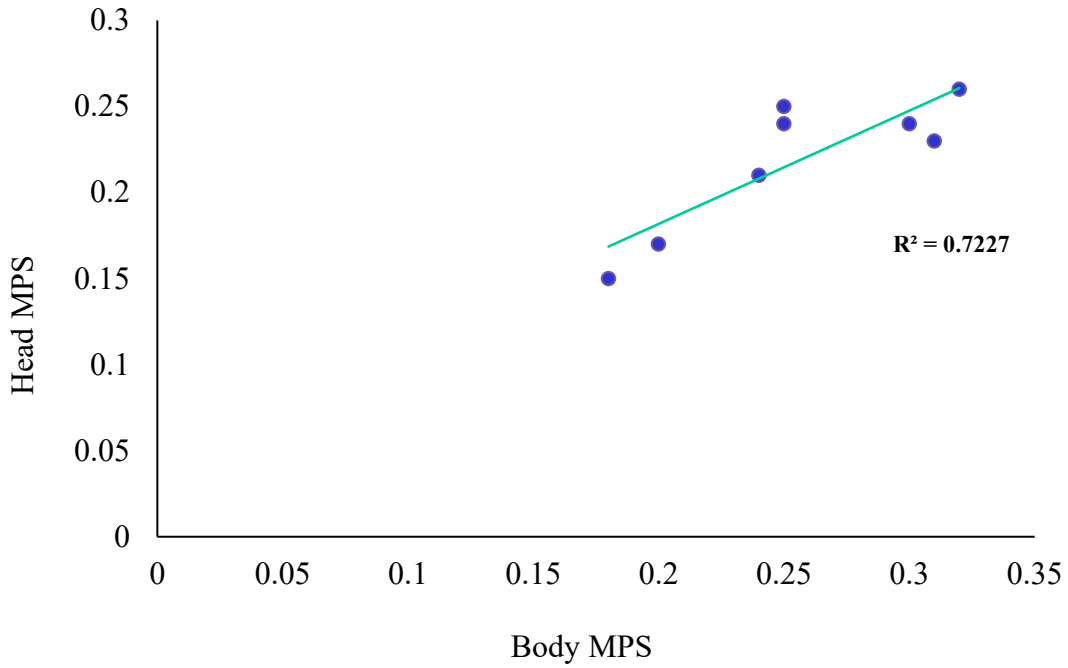

Figure 17. *Scatterplot and regression line demonstrating the relationship between head and body MPS for glass events*

4.5 – Boards

For the head tracking method, head-to-boards impacts were reconstructed using the monorail drop rig with a high-density polyethylene base supported by a flat steel anvil (Table 7). Impacts were delivered to the right & left side and rear locations and the velocities ranged from 1.64 m/s to 6.05 m/s. The MPS values ranged from 30% to 82%, all of which fell within the high or very high categories (Table 21).

For the body tracking method, the same impacts were reconstructed using the monorail drop rig with a flat MEP anvil (Table 7). Impacts were delivered to the side and rear locations at velocities ranging from 2.88 m/s to 6.48 m/s. The MPS values ranged from 29% to 77% and the categories remained unchanged (Table 21).

The average velocities for the head and body tracking methods were 3.94 m/s and 4.63 m/s, respectively. The average difference in velocity for the two methods was 0.70 m/s (Table 19). The dynamic responses for all boards impacts can be found in Table 20. The average MPS values for the head and body tracking methods were 0.51 and 0.50, respectively (Table 21 and Figure 18). The two methods demonstrated a significant and perfect level of agreement (100%) between MPS categories, with a weighted Cohen's kappa value of 1.00 (p = .01) (Table 9). Boards events demonstrated a significant linear relationship between head and body MPS data and had an R^2 value of .94 ($F(1, 4) = 67.63$, p = .001) (Figure 19).

Table 19. *Average difference in velocity between the head and body tracking reconstruction methods for boards impacts*

Event	Head Velocity (m/s)	Body Velocity (m/s)	Difference (m/s)
Boards 1	1.64	2.88	1.25
Boards 2	2.30	2.81	0.52
Boards 3	3.54	4.52	0.98
Boards 4	4.34	4.52	0.19
Boards 5	5.76	6.56	0.80
Boards 6	6.05	6.48	0.43
Average	**3.94**	**4.63**	**0.70**

Table 20. *Impact locations, velocities, and linear and rotational accelerations for boards impacts reconstructed using the head and body tracking data collection methods*

Event	Head				Body			
	Location	Velocity (m/s)	Linear Acceleration (g)	Rotational Acceleration (rad/s^2)	Location	Velocity (m/s)	Linear Acceleration (g)	Rotational Acceleration (rad/s^2)
Boards 1	Rear	1.64	44.97	2008.17	Rear	2.88	60.13	1175.00
Boards 2	Rear	2.30	49.23	2853.83	Rear	2.81	56.97	1036.90
Boards 3	Right Side	3.54	71.27	2987.57	Side	4.52	103.27	5945.43
Boards 4	Left Side	4.34	86.53	4456.57	Side	4.52	117.87	5633.03
Boards 5	Rear	5.76	185.13	7501.63	Rear	6.56	177.17	7409.97
Boards 6	Left Side	6.05	296.47	18381.93	Side	6.48	227.20	15030.30

Table 21. *MPS values and categories obtained from FE analysis of boards impacts*

Event	Head		Body	
	MPS	MPS Category	MPS	MPS Category
Boards 1	0.30	High	0.29	High
Boards 2	0.32	High	0.27	High
Boards 3	0.42	Very High	0.50	Very High
Boards 4	0.52	Very High	0.48	Very High
Boards 5	0.69	Very High	0.67	Very High
Boards 6	0.82	Very High	0.77	Very High
Average	0.51	-	0.50	-

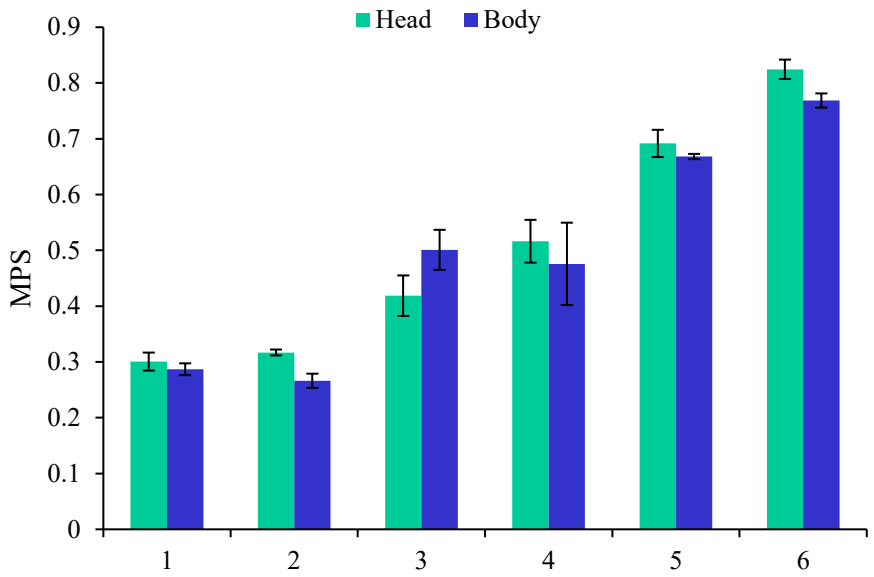

Figure 18. *MPS magnitudes obtained using the UCDBTM V2.0 for boards impacts reconstructed using parameters obtained from head and body tracking; error bars represent the standard deviation of the three reconstruction trials performed for each event*

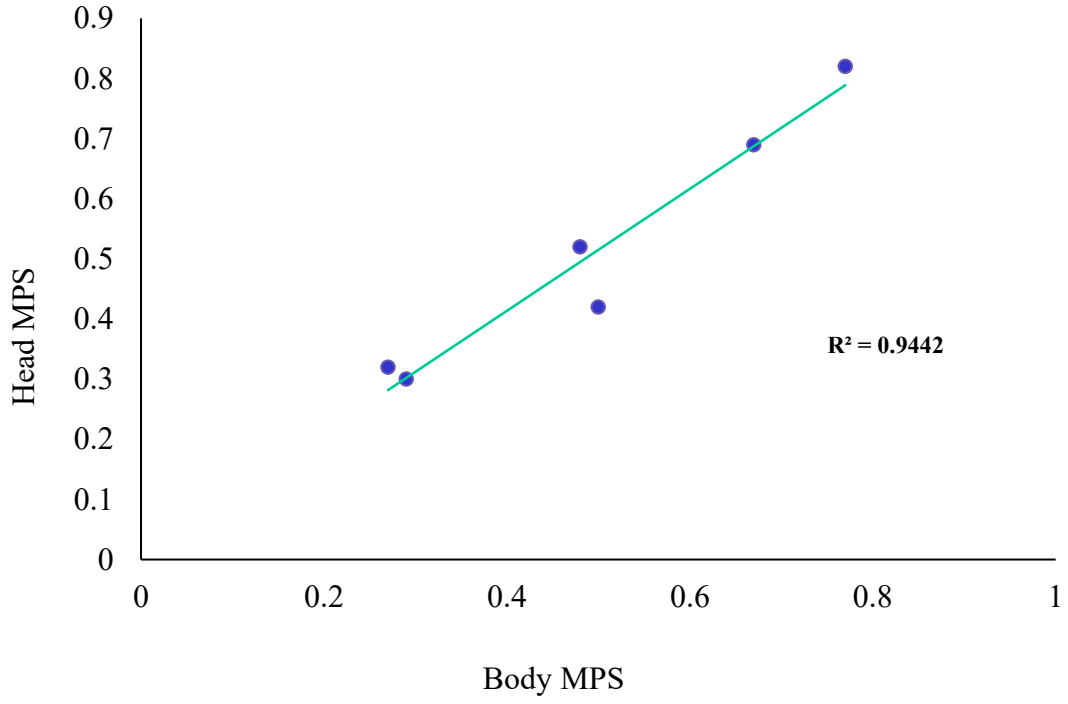

Figure 19. *Scatterplot and regression line demonstrating the relationship between head and body MPS for boards events*

4.6 – Ice

For the head tracking method, ice impacts were reconstructed using the monorail drop rig with an ice anvil (Table 8). Impacts were delivered to the right & left side, rear, and front boss locations and the velocities ranged from 3.39 m/s to 5.06 m/s. The MPS values ranges from 34% to 63%, all of which fell within the very high category except for Ice 1, which corresponded with the high category (Table 24).

For the body tracking method, the same impacts were reconstructed using the monorail drop rig with a flat MEP anvil (Table 8). Impacts were delivered to the side, rear, and front locations and the velocities ranged from 4.37 m/s to 5.19 m/s. The MPS values ranged from 49% to 54%, and all impacts fell within the very high MPS category (Table 24).

The average velocities for the head and body tracking methods were 4.08 m/s and 4.65 m/s, respectively. The average difference in velocity for the two methods was 0.57 m/s (Table 22). The dynamic responses for all ice impacts can be found in Table 23. The average MPS values for the head and body tracking methods were 0.50 and 0.55, respectively (Table 24 and Figure 20). Ice events did not demonstrate a statistically significant level of agreement (86%) between MPS categories for the two methods ($\kappa = .00$, $p = 1.00$) (Table 9). Ice events did not demonstrate a significant linear relationship between head and body MPS data and had an R^2 value of .24 ($F(1, 5) = 1.56$, $p = .27$) (Figure 21).

Table 22. *Average difference in velocity between the head and body tracking reconstruction methods for ice impacts*

Event	Head Velocity (m/s)	Body Velocity (m/s)	Difference (m/s)
Ice 1	3.39	4.37	0.98
Ice 2	3.48	3.91	0.43
Ice 3	3.65	4.07	0.42
Ice 4	4.07	4.96	0.89
Ice 5	4.33	4.80	0.47
Ice 6	4.55	5.25	0.70
Ice 7	5.06	5.19	0.13
Average	**4.08**	**4.65**	**0.57**

Table 23. *Impact locations, velocities, and linear and rotational accelerations for ice impacts reconstructed using the head and body tracking data collection methods*

Event	Head				Body			
	Location	Velocity (m/s)	Linear Acceleration (g)	Rotational Acceleration (rad/s^2)	Location	Velocity (m/s)	Linear Acceleration (g)	Rotational Acceleration (rad/s^2)
Ice 1	Rear	3.39	58.57	2857.90	Rear	4.37	91.23	4122.43
Ice 2	Rear	3.48	66.57	2901.80	Rear	3.91	64.60	2646.60
Ice 3	Front Boss	3.65	194.60	9462.60	Front	4.07	164.33	5874.50
Ice 4	Right Side	4.07	106.87	8807.90	Side	4.96	136.50	8772.17
Ice 5	Rear	4.33	128.93	6204.27	Rear	4.80	115.57	3952.27
Ice 6	Left Side	4.55	95.17	9223.97	Side	5.25	157.80	9409.40
Ice 7	Rear	5.06	138.53	5351.23	Rear	5.19	120.63	3518.87

Table 24. *MPS values and categories obtained from FE analysis of ice impacts*

Event	Head		Body	
	MPS	**MPS Category**	**MPS**	**MPS Category**
Ice 1	0.34	High	0.49	Very High
Ice 2	0.40	Very High	0.39	Very High
Ice 3	0.64	Very High	0.68	Very High
Ice 4	0.40	Very High	0.54	Very High
Ice 5	0.64	Very High	0.54	Very High
Ice 6	0.47	Very High	0.67	Very High
Ice 7	0.63	Very High	0.54	Very High
Average	0.50	-	0.55	-

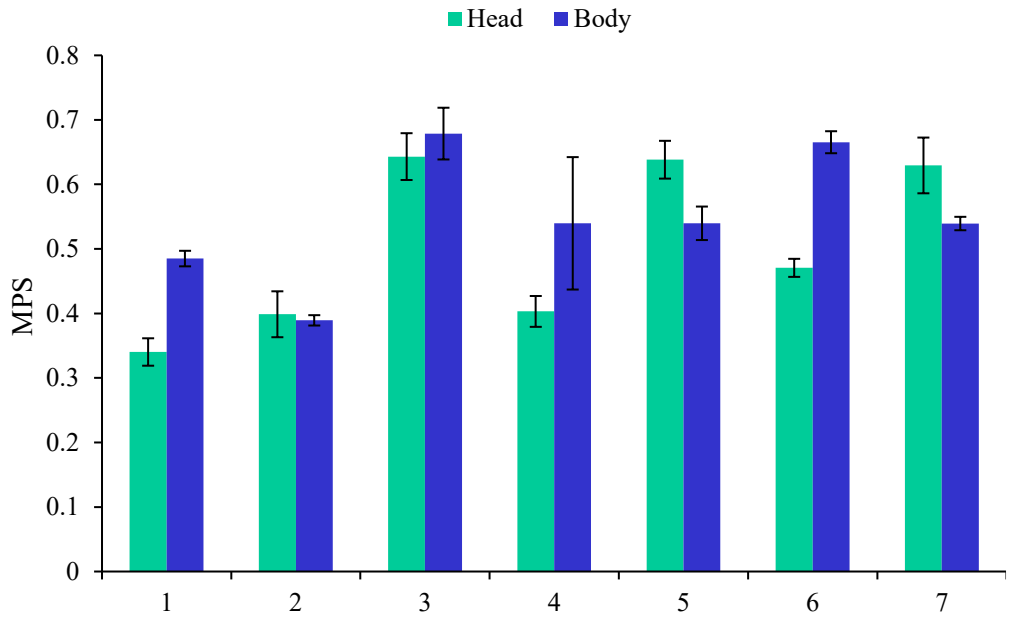

Figure 20. *MPS magnitudes obtained using the UCDBTM V2.0 for ice impacts reconstructed using parameters obtained from head and body tracking; error bars represent the standard deviation of the three reconstruction trials performed for each event*

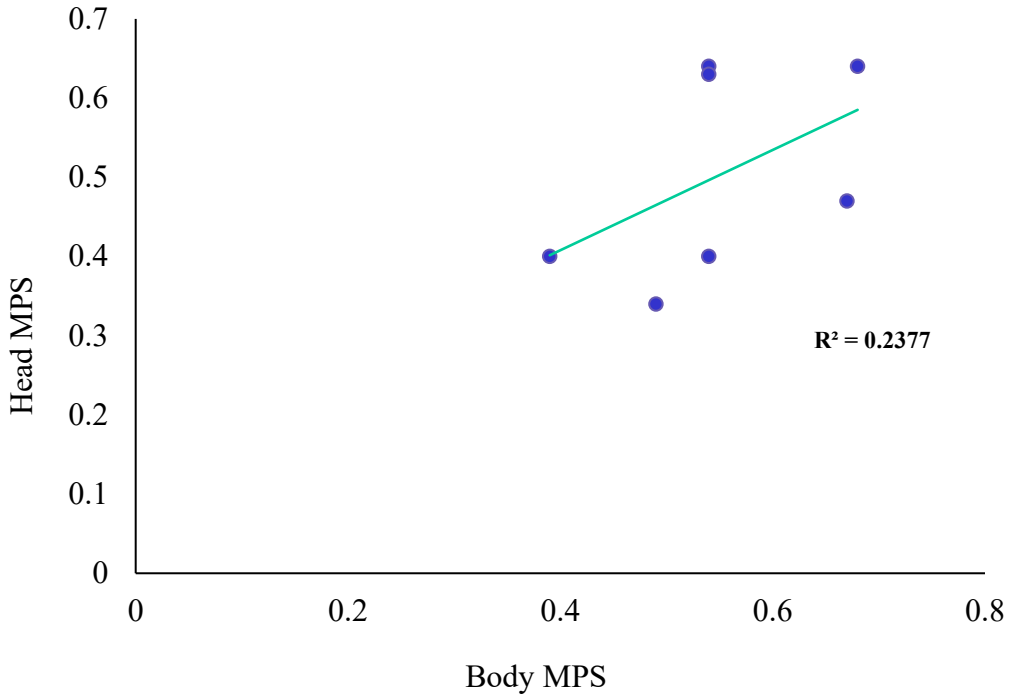

Figure 21. *Scatterplot and regression line demonstrating the relationship between head and body MPS for ice events*

Chapter 5: Discussion

The purpose of this study was to determine whether impact parameters obtained from body tracking can be used to obtain accurate measures of brain strain. The two data collection methods were compared to examine the sensitivity of the kinematic data obtained using body tracking and identify which impact parameters are the most influential in measuring magnitude.

5.1 – Head vs. Body Tracking

Maximum principal strain has been identified as being one of the greatest descriptors of the relative risk of brain injury (Willinger & Baumgartner, 2003; Zhang et al., 2004; Kleiven, 2007; Oeur et al., 2015). When all events were collapsed, the head and body tracking methods demonstrated a strong and significant linear relationship. When analyzed by event type, shoulder and glass events demonstrated significant differences in MPS magnitudes for the two methods. The level of agreement between MPS categories was assessed using weighted Cohen's kappa, which provides a chance-corrected index of IRA/IRR (interrater agreement and interrater reliability) (Gisev et al., 2013). The overall kappa value of 0.56 represents moderate agreement between MPS categories (Landis & Koch, 1977).

5.2 – Shoulder and Elbow

The head tracking method used to reconstruct shoulder impacts was based on research performed by De Grau and colleagues (2020b) who tested the protective capacity of ice hockey helmets at different levels of striking compliance. The high compliance striker was used to produce acceleration pulse durations of 25 ms, which correspond with shoulder impacts that characteristically result in durations of 20 ms or greater (Post et al., 2019a). The pendulum system was used to reconstruct elbow events, which vary in their impact durations (10-28 ms) (Rousseau, 2014; Post et al., 2019a; De Grau et al., 2020a). Analyzing NHL collisions,

Hutchison (2011) demonstrated that elbow-to-head impacts account for approximately 23% of all concussion cases. The head tracking method was based on research conducted by Post and colleagues (2019b), who used the pendulum to reconstruct elbow-to-head impacts delivered from Novice and Midget ice hockey players. Compared to the linear impactor, the pendulum is more representative of the swinging motion of the elbow during an impact. However, the pendulum also allows greater degrees of freedom of the impact event, which may have contributed to the increased measurement variability (Karton et al., 2014). Additionally, the effective mass of the pendulum (~3.9 kg) differs from the linear impactor (13.1 kg) – and this is the only event that used different test equipment for the two methods (Post et al., 2019b). A striking mass below 10 kg has been attributed to an increase in head form acceleration, which has a significant effect on resulting MPS (Karton et al., 2014).

During hockey impacts, impact compliance is affected by the various contacting surfaces found in a standard ice hockey rink. In addition to these surfaces, protective padding and helmets affect energy transfer to the head and create different event durations (Post et al., 2019a). It was assumed that an automated body tracking data capture method would not be able to differentiate between shoulder and elbow impacts, as these body parts are smaller than the body (as a unit) and may not be visible from video depending on the camera view and player location. Shoulder and elbow impacts also represent similar mechanisms of injury and result in similar impact durations (Rousseau, 2014; Post et al., 2019a; De Grau et al., 2020a). These event types were grouped together for body tracking reconstructions to determine whether compliance can be made more refined yet produce similar measures of brain strain magnitude to the standard head tracking method. However, the medium compliance striker cap used for the body tracking reconstructions was more representative of elbow impacts ($R^2 = .7144$, $F(1, 5) = 12.51$, $p = .02$)

compared to shoulder impacts, which were reconstructed using the high compliance striker cap for the head tracking method. Therefore, the R^2 value (R^2 = .6647, $F(1, 6) = 11.90$, $p = .01$), significant difference in strain magnitudes, and poor agreement between MPS categories for shoulder events were attributed to the difference in compliance for the head and body tracking reconstructions. Research has shown that increased material compression increases the duration of the impact event, thus affecting the dynamic response and resulting MPS (De Grau et al., 2020a). Studies that have analyzed the effects of surface compliance on brain strain have clearly demonstrated that changes in duration can have significant effects on MPS (Oeur et al., 2018; Post et al., 2019a; De Grau et al., 2020a; 2020b).

5.3 – Glass

Compared to player collisions, impacts to glass create different loading characteristics that affect brain tissue kinematics and strains (Post et al., 2019a). The same test equipment was used for both head and body tracking reconstructions, therefore unlike the shoulder and elbow event types, compliance would not have influenced the relationship between the two methods. Except for the boards, the average difference in velocity (0.70 m/s) between the head and body tracking methods was greater than the other event types. Since velocity was the parameter that varied the most, the narrow range of velocities used for glass reconstructions (3.08 – 5.25 m/s) could explain the R^2 of .7227 ($F(1, 6) = 15.64$, $p = .008$) and the significant difference in MPS magnitudes for the head and body tracking methods.

5.4 – Boards and Ice

Hockey has been identified as one of world's fastest contact sports, as players have the ability reach high velocities due to the low friction between the ice and skates (De Grau et al., 2020a). Current ice hockey helmet technologies are primarily designed to manage short duration high-magnitude events, such as falls to the ice or crashes into the boards (Hoshizaki et al., 2014; Hoshizaki et al., 2017). On average, these events produce the highest levels of strain (42%) compared to those resulting from impacts caused by collisions (31%), projectiles (14%), and punches (23%) (Hoshizaki et al., 2014). Head impacts that result in MPS magnitudes of 26% and above have been reported as 'extreme' hits that often elicit concussive-like symptoms (Pellman et al., 2004; Campbell, 2014; Karton et al., 2020). The energy-absorbing material within a helmet is designed to perform within a designated energy range (Hoshizaki & Brien, 2004). In high-energy impacts, the energy-absorbing material almost undergoes complete compression and the severity of the impact increases greatly (Hutchison, 2014). The ice events chosen for this study were very high energy impacts, with players hitting rigid surfaces at high velocities. Similar to the shoulder and elbow events, boards and ice were grouped together for the body tracking reconstructions because they also represent similar mechanisms of injury and produce similar impact durations (Post et al., 2019a; Meehan, 2019). The MEP anvil used for the body tracking reconstructions was representative of the surface compliance for both the boards and ice, as it is composed of stiff materials that offer very little compliance and are the least influential on results in terms of energy absorption (Karton et al., 2014). Compared to the boards (R^2 = .9442, $F(1, 4) = 67.63$, $p = .001$), ice events did not demonstrate a significant relationship or level of agreement between head and body tracking MPS magnitudes and categories because a narrow range of high energy impacts were analyzed. These impacts did not elicit major response

changes, resulting in a small distribution and low R^2 = .2377 ($F(1, 5) = 1.56$, p = .267). In addition, every MPS value obtained using the body tracking method fell within the very high MPS category, while only one MPS value obtained using the head tracking method fell within the high MPS category (Ice 1). Despite having an 86% agreement, ice impacts had a weighted Cohen's kappa value of 0.00 (p = 1.00) which was due to the large imbalance in MPS categories for these events (Feinstein & Cicchetti, 1990).

5.5 – Limitations and Future Research

The methods presented in this study included some limitations. The difference in compliance between the two methods used to reconstruct head-to-shoulder events made it challenging to compare resulting MPS values and categories. While shoulder impacts resulted in a large range of acceleration pulses that were similar in duration to those of elbow impacts (Rousseau, 2014; Post et al., 2019; Meehan, 2019; De Grau et al., 2020a), these events should be considered separately. A discrepancy in velocity measurements was also noted between the two methods. This difference (0.58 m/s) was likely due to the orientation of the body pre-impact, as the head could have been closer than the body tracking reference point (center of the sternum, scapulae, or glenohumeral joint) to the impact location. Players have the tendency to be in an upright position when they collide, whereas their bodies are often flexed or bent over during a fall to the ice or crash into the boards. In real life, the head and body should be moving simultaneously and there should not be a significant difference in displacement measurements. However, calculating velocity (displacement/time) using Kinovea requires the distance measured between the impact location of the head or body to the contacting surface (shoulder, elbow, glass, boards, or ice). To avoid errors in velocity measurements, trials using a validated player tracking software should be conducted to confirm the exact velocity of the impact. Another

limitation involved the use of different test equipment to reconstruct elbow-to-head impacts, which could have influenced the results due to discrepancies in mass and the manner in which they were delivered. When conducting a direct comparison between two methods, this research demonstrated the importance of using the same mechanical system (linear impactor, pendulum, monorail drop rig) for head impact reconstructions. For boards and ice impacts, velocities below 1.64 m/s were not analyzed. A greater difference between MPS values and categories may have been observed if lower-velocity impacts were analyzed, such as in a youth ice hockey game. Future studies should incorporate various sports and levels of play to determine whether this method could be applied universally.

Chapter 6: Conclusion

The purpose of this research was to determine if impact variables obtained by video analysis and event reconstruction using impact characteristics obtained from body tracking could yield similar measures of strain magnitude to those obtained using head tracking. The differences between head and body tracking methods were predominantly affected by velocity and compliance. Overall, the results demonstrated a significant difference between the MPS magnitudes obtained using impact parameters from body and head tracking data from 2D video. Shoulder and glass events demonstrated significant differences in MPS magnitudes, which were attributed to a discrepancy in compliance and a greater difference in velocity measurements between the two methods. Ice events did not demonstrate a significant linear relationship between head and body MPS, which was attributed to a narrow range of analyzed responses. The two methods demonstrated a perfect level of agreement (100%) between MPS categories for boards impacts and a moderate level of agreement (56%) overall. A strong linear relationship between the head and body tracking methods was depicted, demonstrating that impact characteristics obtained from body tracking and 2D video can be used to measure brain tissue strain. Effective management of head trauma in sport requires an objective, accessible, and quantifiable tool to overcome the limitations associated with current measures. This method provides the basis for developing an automated data capture tool that can measure the entire spectrum of brain trauma. By combining body tracking data and event reconstruction, impact magnitude can be determined rapidly and effectively, creating a simplified and universal opportunity to measure and manage the entire spectrum of brain trauma at all levels of competition.

References

Bailey, A., Funk, J., Lessley, D., Sherwood, C., Crandall, J., Neale, W., and Rose, N. 2020. Vallidation of a videogrammetry technique for analysing American football helmet kinematics. Sports Biomech. 19 (5): 678-700

Bain, A., and Meaney, D. 2000. Tissue-level thresholds for axonal damage in an experimental model of central nervous system white matter injury. J. Biomech. 122: 615-622

Beckwith, J. G., Chu, J. J., and Greenwald, R. M. 2007. Validation of a noninvasive system for measuring head acceleration for use during boxing competition. J. Appl. Biomech. 23: 238-244

Broglio, S. P., Eckner, J. T., Paulson, H. L., and Kutcher, J. S. 2012. Cognitive decline and aging: the role of concussive and subconcussive impacts. Exerc. Sport. Sci. Rev. 40 (3): 138-144

Buchheit, M., Allen, A., Poon, T. K., Modonutti, M., Gregson, W., and Di Salvo, V. 2014. Integrating different tracking systems in football: multiple camera semi-automatic system, local position measurement and GPS technologies. J. Sports Sci. 32(20): 1844-1857

Campbell, K. 2014. Quantifying and comparing head impact biomechanics of different player positions for Canadian University football. Master's Thesis, Western University, London, ON, Canada

Canadian Standards Association. 2015. Ice hockey helmets. CAN/CSA Z262.1-15. Mississauga, ON, Canadac

CCM Hockey. 2021. CCM all out: Tacks 110 combo helmet senior. Sport Maska Inc. https://ca.ccmhockey.com/Sale/HT110C-SR.html

Choe, M. C. Babikian, T., DiFiori, J., Hovda, D. A., and Giza, C. C. 2012. A pediatric perspective on concussion pathophysiology. Curr. Opin. Pediatr. 24(6): 689-695

Clark, J. M., Post, A. Hoshizaki, T. B. and Gilchrist, M. D. 2015. Determining the relationship between linear and rotational acceleration and MPS for different magnitudes of classified brain injury risk in ice hockey. IRCOBI Conference 2015 (IRC-15-26)

Clark, J. M., Post, A., Hoshizaki, T. B., and Gilchrist, M. D. 2016. Protective capacity of ice hockey helmets against different impact events. Ann. Biomed. Eng. 44 (12): 3693-3704

Clark, J. M., Adanty, K., Post, A., Hoshizaki, T. B., Clissold, J., McGoldrick, A., Annaidh, A., and Gilchrist, M. D. 2018a. Reconstruction of real world concussive and non-concussive accidents in equestrian sports. IRCOBI Conference 2018 (IRC-18-47)

Clark, J. M., Taylor, K., Post, A., Hoshizaki, T. B., Gilchrist, M. D. 2018b. Comparison of ice hockey goaltender helmets for concussion type impacts. Ann. Biomed. Eng. 46 (7): 986-1000

Clark, J. M., Connor, T., Post, A., Hoshizaki, T. B., and Gilchrist, M. D. 2021. The influence of impact surface on head kinematics and brain tissue response during impacts with equestrian helmets. Sports Biomech. 20(6): 737-750

Cotsonika, N. 2020. Puck, player tracking in final testing stage before Stanley Cup Playoffs. Obtained from: https://www.nhl.com/news/puck-player-tracking-technology-unveiled-during-2020-postseason/c-315806398

Davis, J., Sharma, V., Tyagi, A., and Keck, M. 2009. Human detection and tracking. In: Encyclopedia of Biometrics. Boston, MA. Springer, S. Li and A. Jain, Eds. 978-0-387-73003-5

De Grau, S., Post, A., Hoshizaki, T. B., and Gilchrist, M. 2020a. Effects of surface compliance on the dynamic response and strains sustained by a player's helmeted head during ice hockey impacts. Proc. Inst. Mech. Eng. Pt. P J. Sports Eng. Tech. 234(4): 98-106

De Grau, S., Post, A., Meehan, A., Champoux, L., Hoshizaki, T. B., and Gilchrist, M. 2020b. Protective capacity of ice hockey helmets at different levels of striking compliance. Sports Eng. 23(11): 1-10

Defroda, S., Thigpen, C. A., and Kriz, P. K. 2016. Two-dimensional video analysis of youth and adolescent pitching biomechanics: a tool for the common athlete. Curr. Sports Med. Rep.15(5): 350-358

Doorly, M.C., Gilchrist, M. D. 2006. The use of accident reconstruction for the analysis of traumatic brain injury due to head impacts arising from falls. Comput. Methods Biomech. Biomed. Engin. 9: 371–37

Doorly, M.C., Gilchrist, M. D. 2009. Three-dimensional multibody dynamics analysis of accidental falls resulting in traumatic brain injury. Int. J. Crashworthiness. 14: 503–509

Elkin, B. S., and Morrison 3rd, B. 2007. Region-specific tolerance criteria for the living brain. Stapp. Car Crash J. 51: 127-138

Elkin, B. S., Gabler, L. F., Panzer, M. B., and Siegmund, G. P. 2018. Brain tissue strains vary with head impact location: A possible explanation for increased concussion risk in struck versus striking football players. Clin. Biomech. 64: 49-57

Fahlstedt, M., Baeck, K., Halldin, P., Van Der Sloten, J., Goffin, J., Depreitere, B., and Kleiven, S. 2012. Influence of impact velocity and angle in a detailed reconstruction of a bicycle accident. IRCOBI Conference 2012 (IRC-12-84)

Feinstein, A., and Cicchetti, D. 1990. High agreement but low kappa: I. The problems of two paradoxes. J. Clin. Epidemiol. 43(6): 543-549

Forero Rueda, M. A., Cui, L., and Gilchrist, M. D. 2011. Finite element modelling of equestrian helmet impacts exposes the need to address rotational kinematics in future helmet designs. 14 (12): 1021-1031

Gennarelli, T. A., Thibault, L., Adams, H., Graham, D., Thompson, C. J., and Marcincin, R. P. 1982. Diffuse axonal injury and traumatic coma in the primate. Ann. Neurol. 12: 564–574

Gennarelli, T. 1983. Head injury in man and experimental animals: clinical aspects. Acta. Neurochir. Suppl. 32: 1-13

Gennarelli, T. A., Lawrence, E., Thibault, G., Tomei, R., Wiser, D., Graham, D., and Adams, J. 1987. Directional dependence of axonal brain injury due to centroidal and non-centroidal acceleration. SAE Technical Paper 872197: 49–53

Gilchrist, M. D. 2003. Modelling and accident reconstruction of head impact injuries. Key. Eng. Mat. 245: 417-430

Gioia, G. A. 2015. Multimodal evaluation and management of children with concussion: using out heads and available evidence. Brain Inj. 29: 195-206

Giordano, C., and Kleiven, S. 2014. Evaluation of axonal strain as a predictor for mild traumatic brain injuries using finite element modeling. Stapp Car Crash J. 58: 29-61

Gisev, N., Bell, J. S., and Chen, T. 2013. Interrater agreement and interrater reliability: Key concepts, approaches, and applications. Res. Social Adm. Pharm. 9: 330-338

Giza, C. C. 2014. Pediatric issues in sports concussions. Continuum: Lifelong Learning in Neurology. Sports Neurol. 20: 1570-1587

Graham, R. 2014. Concussion recognition, diagnosis, and acute management. In: Sports-Related Concussions in Youth: Improving the Science, Changing the Culture. Washington, DC: National Academies Press (US), R. Graham, F. P. Rivara, M. A. Ford, et al., Eds. 99-180

Greenbaum, D. 2018. Wuz you robbed? Concerns with using big data analytics in sports. Am. J. Bioeth. 18(6): 32-33

Gyemi, D., Andrews, D., and Jadischke, R. 2021. Three-dimensional video analysis of helmet-to-ground impacts in North American youth football. J. Biomech. 125: 110587

Hanlon, E., and Bir, C. 2010. Validation of a wireless head acceleration measurement system for use in soccer play. J. Appl. Biomech. 26: 424-431

Hardy, W., Foster, C., Mason, M., Yang, K., King, A., and Tashman, S. 2001. Investigation of head injury mechanisms using neutral density technology and high-speed biplanar X-ray. Stapp. Car Crash J. 45: 337-368

Hardy, W., Mason, M., Foster, C., Shah, C., Kopacz, J., Yang, K., King, A., Bishop, J., Bey, M., Anderst, W., and Tashman, S. 2007. A study of the response of the human cadaver head to impact. Stapp. Car Crash J. 51: 17

Hoshizaki, T.B., and Brien, S.F. 2004. The science and design of head protection in sport. Neurosurg. 55: 956-967

Hoshizaki, T. B., Post, A., Oeur, R. A., and Brien, S. 2014. Current and future concepts in helmet and sports injury prevention. Neurosurg. 75 (4): S136-S148

Hoshizaki, T. B., Post, A, Kendall, M., Cournoyer, J., Rousseau, P., Gilchrist, M. D., Brien, S., Cusimano, M., and Marshall, S. 2017. The development of a threshold curve for the understanding of concussion in sport. Trauma.19(3): 196–206

Hua, Y., Akula, P., Kelso, M., and Gu, L. 2015. Characterization of closed head impact injury in rat. Biomed. Res. Int. 1-9

Hutchison, M. 2011. Concussion in the National Hockey League (NHL): The video analysis project. PhD Thesis, University of Toronto, ON, Canada

Hutchison, T. 2014. Peak acceleration during impact with helmet materials: Effects of impactor mass and speed. Eur. J. Sport Sci. 14 (S1): S377-S382

Hutchison, M., Comper, P., Meeuwisse, W., and Echemendia, R. 2015a. A systematic video analysis of National Hockey League (NHL) concussions, part I: who, when, where and what? Br. J. Sports Med. 49(8): 547-551

Hutchison, M., Comper, P., Meeuwisse, W., and Echemendia, R. 2015b. A systematic video analysis of National Hockey League (NHL) concussions, part II: how concussions occur in the NHL. Br. J. Sports Med. 49(8): 552-555

Ignacy, T. 2017. Biomechanics of injury events associated with diagnosed concussion in professional men's rugby league. MSc Thesis, University of Ottawa, Ottawa, ON, Canada

Karton, C., Hoshizaki, T. B., and Gilchrist, M. D. 2014. The influence of impactor mass on the dynamic response of the Hybrid III headform and brain tissue deformation. In: Mechanism of Concussion in Sports. Atlanta, GA. ASTM International, A. Ashare and M. Ziejewski, Eds. 23–40

Karton, C., and Hoshizaki, T. B. 2018. Concussive and subconcussive brain trauma: the complexity of impact biomechanics and injury risk in contact sport. In: Handbook of Clinical Neurology, Volume 158 (3rd series), Sports Neurology, B. Hainline and R.A. Stern, Eds. 39-49

Karton, C., Hoshizaki, T. B., and Gilchrist, M. D. 2020. A novel repetitive head impact exposure measurement tool differentiates player position in National Football League. Sci. Rep. 10 (1200): 1-14

Karton, C., Post, A., Laflamme, Y., Kendall, M., Cournoyer, J., Robidoux, M., Gilchrist, M. D., and Hoshizaki, T. B. 2021. Exposure to brain trauma in six age divisions of minor ice hockey. J. Biomech. 116: 110203

Kelley, M., Urban, J., Jones, D., Davenport, E., Miller, L., Snively, B., Powers, A., Whitlow, C., Maldjian, J., and Stitzel, J. 2021. Analysis of longitudinal head impact exposure and white matter integrity in returning youth football players. J. Neurosurg. Pediatr. 1-10

Kendall, M., Post, A., Rousseau, P., Oeur, A., Gilchrist, M. D., and Hoshizaki, T. B. 2012a. A comparison of dynamic impact response and brain tissue deformation of head impact reconstructions representing three mechanisms of head injury in ice hockey. IRCOBI Conference 2012 (IRC-12-53)

Kendall, M., Walsh, E., and Hoshizaki, T. B. 2012b. Comparison between Hybrid III and Hodgson-WSU headforms by linear and angular dynamic impact response. Proc. Inst. Mech. Eng. P: J. Sport Eng. Technol. 226 (3/4): 260-265

Kimpara, H., and Iwamoto, M. 2011. Mild traumatic brain injury predictors based on angular accelerations during impacts. Ann. Biomed. Eng. 40(1): 114–126

King, A. I., Yang, K. H., Zhang, L., and Hardy, W. 2003. Is head injury caused by linear or angular acceleration? IRCOBI Conference 2003 (Lisbon, Portugal)

Kleiven, S. 2003. Influence of impact direction to the human head in prediction of subdural haematoma. J. Neurotraum. 20: 365–379

Kleiven, S. 2006. Evaluation of head injury criteria using a finite element model validated against experiments on localized brain motion, intracerebral acceleration, and intracranial pressure. Int. J. Crashworthiness. 11(1): 65–79

Kleiven, S. 2007. Predictors for traumatic brain injuries evaluated through accident reconstruction. Stapp. Car Crash J. 51: 81–114

Kniffin, K., Howley, T. and Bardreau, C. 2017. Putting muscle into sports analytics: strength, conditioning, and ice hockey performance. J. Strength Cond. Res. 31(12): 3253–3259

Kosziwka, G., Champoux, L., Cournoyer, J., Gilchrist, N., and Hoshizaki, T. B. 2021. Risk of head injury associated with distinct head impact events in elite women's ice hockey. J. Concussion. 5: 1-8

Lage, L. 2021. NHL tracking pucks this season, opening up gambling options. Obtained from: https://apnews.com/article/nhl-technology-sports-business-hockey-598b28664151ed1bebacd2e8b31f70d1

Landis, J. R. and Koch, G. G. 1977. The measurement of observer agreement for categorical data. Biometrics. 33: 159-174

Ling, H., Hardy, J., and Zetterberg, H. 2015. Neurological consequences of traumatic brain injuries in sports. Mol. Cell Neurosci. 66(Pt B): 114-122

Loyd, A., Nightingale, R., Song, Y., Luck, J., Cutcliffe, H., Myers, B., and Bass, C. 2014. The response of the adult and ATD heads to impacts onto a rigid surface. Accid. Anal. Prev. 72: 219-229

Margulies, S. S. and Thibault, L. E. 1992. A proposed tolerance criteria for diffuse axonal injury. J. Biomech. 25: 917-923

McAllister, T. and McCrea, M. 2017. Long-term cognitive and neuropsychiatric consequences of repetitive concussion and head impact exposure. J. Athl. Train. 52(3): 309-317

McClelland, K. 2021. Skating Mechanics to Improve Your Speed. Obtained from https://www.hockeytraining.com/skating-lower-body-mechanics/

McKee, A. C., Alosco, M. L., and Huber, B. R. 2016. Repetitive head impacts and chronic traumatic encephalopathy. Neurosurg. Clin. N. Am. 27 (4): 529-535

Meehan, A. 2019. Describing the relationship between three ice hockey helmet impact tests and reconstructions of concussive injuries in professional ice hockey. MSc Thesis, University of Ottawa, Ottawa, ON, Canada

Mihalik, J. P., Bell, D. R., Marshall, S. W., and Guskiewicz, K. M. 2007. Measurement of head impacts in collegiate football players: an investigation of positional and event-type differences. Neurosurg. 61: 1229-1235

Mihalik, J. P., Guskiewicz, K., Marshall, S., Blackburn, J. T., Cantu, R., and Greenwald, R. 2012. Head impact biomechanics in youth hockey: comparisons across playing position, event types, and impact locations. Ann. Biomed. Eng. 40 (1): 141-149

Milne, G., Deck, C., Bourdet, N., Alline, Q., Gallego, A., Carreira, R. P., and Willinger, R. 2013. Assessment of bicyclist head injury risk under tangential impact conditions. IRCOBI Conference 2013 (IRC-13-90)

Montenigro, P., Alosco, M., Martin, B., Daneshvar, D., Mez, J., Chaisson, C., Nowinski, C., Au, R., McKee, A., Cantu, R., McClean, M., Stern, R., and Tripodis, Y. 2017. Cumulative head impact exposure predicts later-life depression, apathy, executive dysfunction, and cognitive impairment in former high school and college football players. J. Neurotrauma. 34 (2): 328-340

O'Riordain, K., Thomas, P. M., Phillips, J. P., Gilchrist, M.D. 2003. Reconstruction of real world head injury accidents resulting from falls using multibody dynamics. Clin. Biomech. 18: 590–60

Oeur, A., Hoshizaki, T. B., and Gilchrist, M.D. 2014. The influence of impact angle on the dynamic response of a Hybrid III headform and brain tissue angle. Mechanism of Concussion in Sports, STP 1552, Alan Ashare and Mariusz Ziejewski, Eds. 56-69

Oeur, A., Karton, C., Post, A., Rousseau, P., Hoshizaki, T. B., Marshall, S., Brien, S., Smith, A., Cusimano, M., and Gilchrist, M. 2015. A comparison of head dynamic response and brain tissue stress and strain using accident reconstructions for concussion, concussion with persistent postconcussive symptoms, and subdural hematoma. J. Neurosurg. 123: 415-422

Oeur, A., Gilchrist, M. D., and Hoshizaki, T. B. 2018. Interaction of impact parameters for simulated falls in sport using three different sized Hybrid III headforms. Int. J. Crashworthiness. 24(3): 326-335

Oeur, A., Gilchrist, M. D., and Hoshizaki, T. B. 2019. Interaction of external head impact parameters on region and volume of strain for collisions in sport. Inst. Mech. Eng. P J. Sport. Eng. Technol. 233(2): 258–267

Ogus, S. 2020. NHL's puck and player tracking technology testes in all-star game; set to be up and running for playoffs. Obtained from: https://www.forbes.com/sites/simonogus/2020/01/28/nhls-puck-and-player-tracking-tested-in-all-star-game-set-to-be-up-and-running-for-playoffs/?sh=615167d9cb57

Ommaya, A. K. 1968. Mechanical properties of tissues of the nervous system. J. Biomech. 1 (2): 127-138

Ommaya, A. K., and Hirsch, A. E. 1971. Tolerances for cerebral concussion from head impact and whiplash in primates. J. Biomech. 4 (1): 13-21

Padgaonkar, A. J., Kreiger, K. W., and King, A. I. 1975. Measurement of angular acceleration of a rigid body using linear accelerometers. J. Appl. Mech. 42:552–556.

Passfield, L. and Hopker J. 2017. A mine of information: can sports analytics provide wisdom from your data? Int. J. Sports Physiol. Perform. 12(7): 851-855

Patton, D. A., McIntosh, A. S., and Kleiven, S. 2015. The biomechanical determinants of concussion: finite element simulations to investigate tissue-level predictors of injury during sporting impacts to the unprotected head. J. Appl. Biomech. 31(4): 264–268

Patton, D. A. 2016. A review of instrumented equipment to investigate head impacts in sport. Appl. Bionics Biomech. 7049743: 1-16

Pellman, E., Viano, D. C., Tucker, Casson, I., Committee on Mild Traumatic Brain Injury, National Football League. 2003a. Concussion in professional football: location and direction of helmet impacts – part 2. Neurosurg. 53(6): 1328–1341

Pellman, E., Viano, D. C., Tucker, A., Casson, I., and Waeckerle, J. 2003b. Concussion in professional football: reconstruction of game impacts and injuries. Neurosurg. 53 (4): 799-814

Pellman, E., Powell, J., Viano, D., Casson, I., Tucker, A., Feuer, H., Lovell, M., Waeckerle, J., and Robertson, D. 2004. Concussion in professional football: Epidemiological features of game injuries and review of the literature – part 3. Neurosurg. 54 (1): 81–96

Post, A. and Hoshizaki, T. B. 2012. Mechanisms of brain impact injuries and their prediction: a review. Trauma. 14: 327–349

Post, A. and Hoshizaki, T. B. 2015. Rotational acceleration, brain tissue strain, and the relationship to concussion. J. Biomech. Eng. 137: 1-8

Post, A., Oeur, A., Hoshizaki, T. B., and Gilchrist, M. D. 2011. Examination of the relationship between peak linear and angular accelerations to brain deformation metrics in hockey helmet impacts. Comput. Methods Biomech. Biomed. Engin. 16 (5): 511-519

Post, A., Hoshizaki, T. B., Gilchrist, M., and Brien, S. 2012. Analysis of the influence of independent variables used for reconstruction of a traumatic brain injury incident. Proc. Inst. Mech. Eng. Pt. P J. Sports Eng. Tech. 226: 290–29

Post, A. Oeur, A., Hoshizaki, T. B., and Gilchrist, M. D. 2013. The influence of velocity on the performance range of American football helmets. 1st International Conference on Helmet Performance and Design. London, UK

Post, A., De Grau, S., Ignacy, T., Meehan, A., Zemek, R., Hoshizaki, T. B., and Gilchrist, M. D. 2016. Comparison of helmeted head impact in youth and adult ice hockey. IRCOBI Conference 2016 (IRC-16-30)

Post, A., Hoshizaki, T. B., Gilchrist, M. D., and Cusimano, M. D. 2017. Peak linear and rotational acceleration magnitude and duration effects on maximum principal strain in the corpus callosum for sport impacts. J. Biomech. 61: 183-192

Post, A., Kendall, M., Cournoyer, J., Karton, C., Oeur, R. A., Dawson, L., and Hoshizaki, T. B. 2018. Brain tissue analysis of impacts to American football helmets. Comput. Methods Biomech. Biomed. Eng. 21(3): 264-277

Post, A., Hoshizaki, T. B., Karton, C., Clark, J. M., Dawson, L., Cournoyer, J., Taylor, K., Oeur, R. A., Gilchrist, M. D., and Cusimano, M. D. 2019a. The biomechanics of concussion for ice hockey head impact events. Comput. Methods Biomech. Biomed. Engin. 22(6): 631-643

Post, A., Karton, C., Robidoux, M., Gilchrist, M., and Hoshizaki, T. B. 2019b. An examination of the brain trauma in Novice and Midget ice hockey: Implications for helmet innovation. 42nd Conference of the Canadian Medical and Biological Engineering Society. Ottawa, ON, Canada

Public Health Agency of Canada. 2019. Understanding and Awareness of Sports-Related Concussions, With a Focus on Youth. Final Report. Retrieved from https://publications.gc.ca/site/eng/9.868630/publication.html

Rein, R. and Memmert, D. 2016. Big data and tactical analysis in elite soccer: future challenges and opportunities for sports science. Springerplus. 5(1410): 1-13

Rousseau, P. 2014. Analysis of concussion metrics of real-world concussive and non-injurious elbow and shoulder to head collisions in ice hockey. PhD Thesis, University of Ottawa, Ottawa, ON, Canada

Rousseau, P., and Hoshizaki, T. B. 2015. Defining the effective impact mass of elbow and shoulder strikes in ice hockey. Sports Biomech. 14(1): 57–67

Rowson, S., Beckwith, J., Chu, J., Leonard, D., Greenwald, R., and Duma, S. 2011. A six degree of freedom head acceleration measurement device for use in football. J. Appl. Biomech. 21(1): 8-14

Rowson, S., Duma, S.M., Beckwith, J.G., Chu, J.J., Greenwald, R.M., Crisco, J.J. Bolinson, P. G., Duhaime, A., McAllister, T., and Maerlender, A. 2012. Rotational head kinematics in football impacts: an injury risk function for concussion. Ann. Biomed. Eng. 40: 1–13

Rowson, B., Tyson, A., Rowson, S., and Duma, S. 2018. Measuring head impacts: accelerometers and other sensors. In: Handbook of Clinical Neurology, Volume 158 (3rd series), Sports Neurology, B. Hainline and R.A. Stern, Eds. 235-243

Russell, K., Ellis, M. J., Bauman, S., and Tator, C. H. 2017. Legislation for youth sport concussion in Canada: review, conceptual framework, and recommendations. Can. J. Neurol. Sci. 44: 225-234

Schussler, E., Stark, D., Bolte, J. H., Kang, Y. S., and Onate, J. A. 2017. Comparison of a head mounted impact measurement device to the Hybrid III anthropomorphic testing device in a controlled laboratory setting. Int. J. Sports Phys. Ther. 12(4): 592-600

Scorza, K., and Cole, W. 2019. Current concepts in concussion: initial evaluation and management. Am. Fam. Physician. 99(7): 426-434

Seidl, T., Czyz, T., Spandler, D., Franke, N., and Lochmann, M. 2016. Validation of football's velocity provided by a radio-based tracking system. 11th conference of the International Sports Engineering Association, ISEA. Procedia Eng. 147: 584 – 589

Shewchenko, N., Withnall, C., Keown, M., Gittens, R., and Dvorak. 2005. Heading in football. Part 1: Development of biomechanical methods to investigate head response. Br. J. Sports Med. 39 (Suppl I): i10–i25

Singh, A., Lu, Y., Chen, C., Kallakuri, S., and Cavanaugh, J. M. 2006. A new model of traumatic axonal injury to determine the effects of strain and displacement rates. Stapp. Car Crash J. 50: 601-623

Tator, C. 2013. Concussions and their consequences: current diagnosis, management and prevention. CMAJ. 185 (11): 975–979

Trotta, A., Clark, J. M., McGoldrick, A., Gilchrist, M. D., and Annaidh, A. 2020. Biofidelic finite element modeling of brain trauma: Importance of the scalp in simulating head impact. Int. J. Mech. Sci. 173: 105448

Walsh, E., and Hoshizaki, T. B. 2010. Sensitivity analysis of a hybrid III head- and neckform to impact angle variations. Procedia Eng. 2 (2): 3487

Walsh, E., Rousseau, P., and Hoshizaki, T. B. 2011. The influence of impact location and angle on the dynamic impact response of a hybrid III headform. Sp. Eng. 13 (3): 135-143

Walsh, E., Post, A., Rousseau, P., Kendall, M., Karton, C., Oeur, A., Foreman, S., and Hoshizaki, T. B. 2012. Dynamic impact response characteristics of a helmeted Hybrid III headform using a centric and non-centric impact protocol. Proc. Inst. Mech. Eng. P: J. Sport Eng. Technol. 226 (3/4): 220-225

Walsh, E., Kendall, M., Post, A., Meehan, A., and Hoshizaki, T. B. 2018. Comparative analysis of Hybrid III neckform and an unbiased neckform. Sports Eng. 21: 479-485

Weaver, A. A., Danelson, K. A., and Stitzel, J. D. 2012. Modeling brain injury response for rotational velocities of varying directions and magnitudes. Ann. Biomed. Eng. 40(9): 2005-2018

Willinger, R., Ryan, G. A., McLean, A. J., Kopp, C. M. 1994. Mechanisms of brain injury related to mathematical modeling and epidemiological data. Accid. Anal. Prev. 26(6): 767-779

Willinger, R., and Baumgartner, D. 2003. Human head tolerance limits to specific injury mechanisms. Int. J. Crashworthiness. 8: 605–617

Yan, E. B., Johnstone, V. P., Alwis, D. S., Morganti-Kossman, M., and Rajan, R. 2013. Characterising effects of impact velocity on brain and behavior in a model of diffuse traumatic axonal injury. Neuroscience. 248: 17-29

Yang, K. H., and King, A. I. 2011. Modeling of the brain for injury simulation and prevention. In: Biomechanics of the Brain, K. Miller, Ed., Springer, 91-110

Zhang, L., Yang, K. H., and King, A. I. 2001. Biomechanics of neurotrauma. Neurol. Res. 23: 144–156

Zhang, L., Yang, K. H., and King, A. I. 2004. A proposed injury threshold for mild traumatic brain injury. J. Biomech. Eng. 126(2): 226–236

Zimmerman, K. A., Kim, J., Karton, C., Lochhead, L., Sharp, D. J., Hoshizaki, T. B., and Ghajari, M. 2021. Player position in American football influences the magnitude of mechanical strains produced in the location of chronic traumatic encephalopathy pathology: A computational modelling study. J. Biomech. 118: 110256

Appendices

Appendix A: Video Analysis

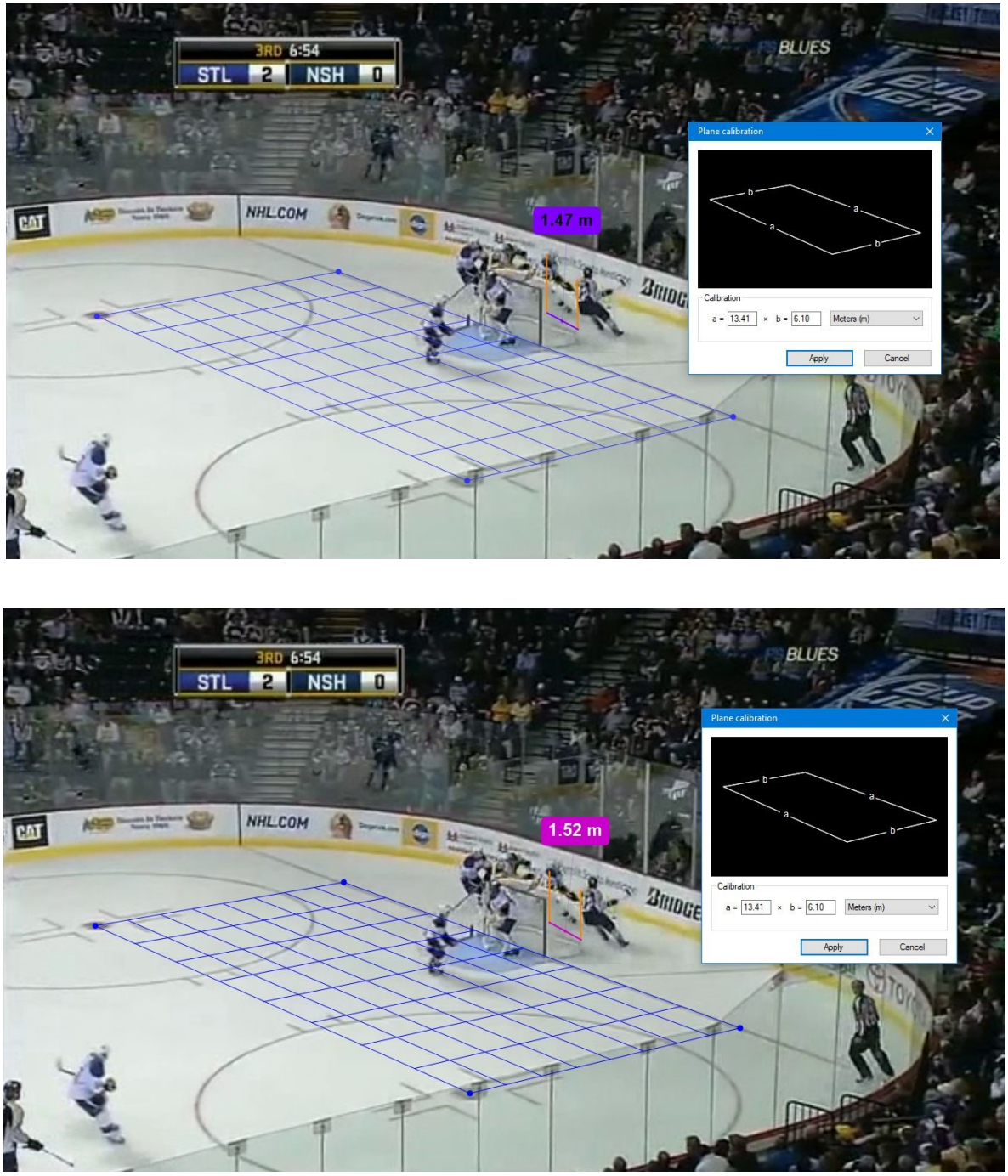

Figure 22. *Kinovea screenshots depicting a collision impact using the head (top) or body tracking reference point (bottom) to calculate velocity*

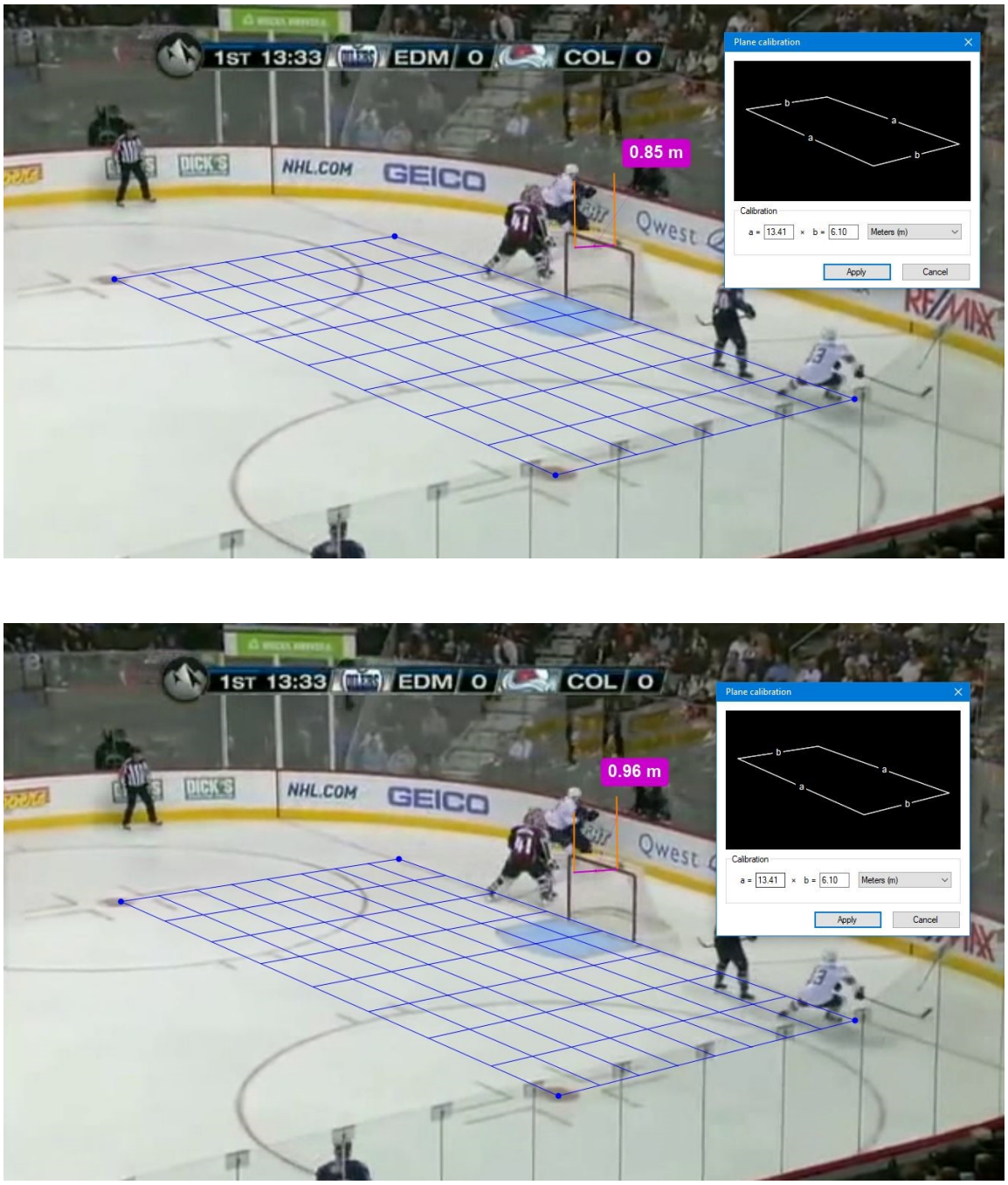

Figure 23. *Kinovea screenshots depicting a glass impact using the head (top) or body tracking reference point (bottom) to calculate velocity*

Figure 24. *Kinovea screenshots depicting an ice impact using the head (top) or body tracking reference point (body) to calculate velocity*

Appendix B: Event Reconstruction

Table 25. *Event grouping criteria based on average durations and MPS values reported in literature*

Event	Literature Reference	Compliance (duration in ms)	MPS
Head-to-ice	Post et al., 2019	10-15	0.43
	Meehan, 2019	13-22.7	0.34
	De Grau et al., 2020a	5.6-10	0.70
Head-to-boards	Post et al., 2019	22-26	0.32
	Meehan, 2019	12.6-23.9	0.40
Head-to-glass	Post et al., 2019	15-20	0.21
Head-to-shoulder	Post et al., 2019	20-35	0.33
	Meehan, 2019	21.0-27.5	0.20
	Rousseau, 2014	18-32	0.30
	De Grau et al., 2020a	21-25.8	0.27
Head-to-elbow	Post et al., 2019	10-28	0.28
	Rousseau, 2014	10-26	0.18
	De Grau et al., 2020a	14-20.6	0.38